Ultrahigh-Temperature Polymers for Second-Order Nonlinear Optics. Synthesis and Properties of Robust, Processable, Chromophore-Embedded Polyimides

M. H. Davey,[†] V. Y. Lee,[‡] L.-M. Wu,[§] C. R. Moylan,[||] W. Volksen,[‡] A. Knoesen,[§] R. D. Miller,*[,‡] and T. J. Marks*[,†]

Department of Chemistry and the Materials Research Center, Northwestern University, 2145 Sheridan Road, Evanston, Illinois 60208-3113; IBM Almaden Research Center, 650 Harry Road, San Jose, California 95120-6099; Organized Research Program on Polymeric Ultrathin Film Systems, Department of Electrical Engineering and Computer Science, University of California, Davis, Davis, California 95616; and Adven Polymers, 1072 South DeAnza Boulevard, San Jose, California 95129

Received July 29, 1999. Revised Manuscript Received March 22, 2000

A general, convergent approach to the synthesis of a series of stilbene- and azo-based donor−acceptor, second-order nonlinear optical (NLO) chromophores is reported. The synthetic strategy enables preparation of both acid- and base-reactive structures, yielding protected, diamine-functionalized chromophores which can be liberated using either acidic or alkaline regents for incorporation into polyimide backbones. Three such chromophores, bis(4-aminophenyl)[4-(2-(4-nitrophenyl)vinyl)phenyl]amine, bis(4-aminophenyl)[4-(2-(6-nitrobenzothiazol-2-yl)vinyl)phenyl]amine, 2-[4-((4-(bis(4-aminophenyl)amino)phenyl)diazenyl)-phenyl]-2-phenyl-1,1-dicyanoethylene, all having high thermal stabilites, were synthesized, characterized, and condensed with hexafluoroisopropylidene diphthalic anhydride or 2-(1,3-dioxoisobenzofuran-5-ylcarbonyloxy)ethyl 1,3-dioxoisobenzofuran-5-carboxylate to yield six high glass transition temperature polyimides (T_g as high as 313 °C) for use as poled NLO materials. After casting as thin films, curing, and electric field corona poling, these materials exhibit $\chi^{(2)}$ (1064 nm) responses as high as 82.0 pm/V and negligible decay in response upon aging in air at 100 °C for over 1000 h.

Introduction

Glassy polymeric materials are of great current scientific and technological interest in nonlinear optics because of ease of processing, large and rapid nonlinear optical (NLO) responses, low dielectric constants, and high laser damage thresholds.[1] While organic NLO materials have been synthesized and studied in many physical forms (e.g., Langmuir−Blodgett films, self-assembled multilayers, vapor deposited films, electric field poled polymers, etc.), poled chromophore-functionalized, glassy macromolecules have received the greatest attention for photonic device applications such as electrooptic modulators and switches.[2]

For new polymeric NLO materials to be practical, several factors must be optimized simultaneously. These include the incorporation of thermally/chemically stable chromophores having large molecular hyperpolarizabilites (β), satisfactory optical transparency, photochemical stability, and straightforward syntheses, while the polymer hosts must exhibit high thermal and oxidative stability, low optical loss, good processability, and low chain segment mobility. Recently, several classes of chromophores with exceptionally large values of $\mu\beta$ have been reported;[3] however, issues such as thermal stability and chemical sensitivity to base, acid, nucleophiles, etc. remain to be resolved. The question of photochemical stability of such high $\mu\beta$ chromophores has only recently been explored;[4] however results to date suggest that such systems may exhibit higher sensitivity to photochemical damage.

Several polymer/chromophore combinations, including those developed in these laboratories,[5] exhibit very high thermal stability (>300 °C), however, frequently suffer from poor processability and modest second-order NLO

[†] Northwestern University.
[‡] IBM Almaden Research Center.
[§] University of California, Davis.
[||] Adven Polymers.

(1) Prasad, P. N.; Williams, D. J. In *Introduction to Nonlinear Optical Effects in Molecules and Polymers*; John Wiley & Sons: New York, 1991.

(2) (a) Burland, D. M.; Miller, R. D.; Walsh, C. A. *Chem. Rev.* **1994**, *94*, 31. (b) Kanis, D. R.; Ratner, M. A.; Marks, T. J. *Chem. Rev.* **1994**, *94*, 195. (c) Dalton, L. R.; Harper, A. W.; Ghosn, R.; Steier, W. H.; Ziari, M.; Fetterman, H.; Shi, Y.; Mustacich, R. V.; Jen, A. K.-Y.; Shea, K. J. *Chem. Mater.* **1995**, *7*, 1060. (d) Marks, T. J.; Ratner, M. *Angew. Chem., Int. Ed. Engl.* **1995**, *34*, 155−173.

(3) (a) Jen, A. K.-Y.; Rao, V. P.; Wong, K. Y.; Drost, K. J. *J. Chem. Soc., Chem. Commun.* **1993**, 90. (b) Rao, V. P.; Jen, A. K.-Y.; Wong, K. Y.; Drost, K. J. *J. Chem. Soc., Chem. Commun.* **1993**, 1118. (c) Jen, A. K.-Y.; Cai, Y.; Bedworth, P. V.; Marder, S. R. *Adv. Mater.* **1997**, *9*, 132. (d) Wang, F.; Ren, A. S.; He, M.; Lee, M. S.; Harper, A. W.; Dalton, L. R.; Zhang, H.; Garner, S. M.; Chen, A.; Steier, W. H. *Polym. Prepr.* **1998**, *39* (2), 1065. (e) Wu, X.; Wu, J.; Liu, Y.; Jen, A. K.-Y. *J. Am. Chem. Soc.* **1999**, *121*, 472. (f) Ren, A. S.; Chen, M.; Lee, M. S.; He, M.; Dalton, L. R.; Zhang, H.; Sun, G.; Garner, S. M.; Steier, W. H. *Polym. Prepr.* **1999**, *40* (1), 160. (g) Albert, I. D. L.; Marks, T.; Ratner, M. A. *J. Am. Chem. Soc.* **1998**, *120*, 11174.

(4) Galvan-Gonzales, A.; Canva, M.; Stegeman, G.; Twieg, R.; Marder, S. Materials Research Symposium, San Francisco, 1999, Abstract F 2.2.

10.1021/cm990483+ CCC: $19.00
Published on Web 05/16/2000

responses. Furthermore, poling at high temperatures is often complicated by increased film electrical conductivity,[6] presumably due, among other factors, to charge injection.[6b,e] The recent work of Jen et al.[7] suggests a chromophore/polymer system which may satisfy many of the aforementioned guidelines. However, a major remaining challenge is actual attachment of the chromophore molecules to a suitable polymeric matrix to produce a material retaining the favorable properties of this guest/host system. Such a task often requires tedious and complex synthetic pathways.

Our studies have focused on two key features of polymeric NLO materials design: (1) understanding how to achieve high thermal stability and orientational stability and (2) developing ways to enhance the ease and generality with which chromophore molecules can be conveniently incorporated into polymeric hosts. With regard to orientational stability in poled polymers,[8] features such as chromophore dimensions, poling methodology, physical aging, chromophore−polymer and chromophore−chromophore interactions, etc., doubtlessly influence the stability of the oriented chromophores. However, it is also clear that polymer chain mobility as expressed by the glass transition temperature (T_g) is of paramount importance,[2] and it has been proposed that a T_g value which is 50 °C or more above the highest continuous device use temperature is necessary to maintain polar order for extended device operation periods.[2a] For on-chip modulators and switches, continuous operating temperatures can be ~80−100 °C, with possible excursions to 250 °C or more for short periods during integration and packaging steps.[9,10] Under these circumstances, the microscopic optical nonlinearity of the material is not the sole concern. Practical materials must display long-term photochemical and thermal stability coupled with orientational stability. The rate of chromophore orientational relaxation depends on many factors. Considerable effort has been expended in an attempt to improve poled polymer orientational stability, including extensive use of in situ network formation.[11] However, the demanding optical loss and dimensional requirements of electrooptic waveguide devices offer significant challenges for crosslinked materials. Furthermore, it has also been recognized that polar order stability can be markedly enhanced in thermoplastic poled polymers by using materials having intrinsically high glass transition temperatures.[5,12] However, efficient exploitation of this approach requires chromophores and polymers with exceptional chemical and thermal stability to permit poling at high temperatures.

Among the high T_g polymer systems attractive for poled second-order materials, functionalized aromatic polyimides offer great potential for addressing the daunting chemical and thermal demands.[5,13] Chromophore design for such systems is nontrivial, and it has been previously reported that dialkylamino donor substituents can seriously compromise high-temperature stability.[14] Furthermore, while flexible alkyl chromophore−polymer tethers facilitate poling by enhancing chromophore mobility, they also tend to lower T_g, adversely affecting orientational stability and may provide a source of thermal and/or chemical instability.

In this contribution, we describe the synthesis and properties of three novel, chemically and thermally stable second-order chromophores as well as their incorporation into the mainchains of six processable polyimides. These chromophores are comprised of aromatic diamines, suitable for incorporation into polyimides, and contain no flexible tethers. The syntheses utilize a convergent approach, allowing facile introduction of various electron-withdrawing groups. The chromophores are directly incorporated into polyimide backbones by straightforward condensation polymerization techniques, resulting in highly rigid, functionalized donor-embedded side chain polyimides having very high T_g values and exceptional thermal stability. The chemical, thermal, microstructural, linear optical, and NLO characterization of these chromophores and the polyimides derived therefrom are described.

Experimental Section

Materials and Measurements. ^{1}H (250 MHz) and ^{13}C (63 MHz) NMR spectra were obtained using a Bruker AC-250 instrument, and chemical shifts are referenced to the internal solvent signal. Melting points are reported as the temperature at the peak of the melting endotherm, measured by differential scanning calorimetry (DSC) using a TA Instruments DSC 2920 (Modulated DSC) at a heating rate of 20 °C/min. Thermogravimetric analyses were conducted using a Perkin-Elmer

(5) (a) Verbiest, T.; Burland, D. M.; Jurich, M. C.; Lee, V. Y.; Miller, R. D.; Volksen, W. *Science* **1995**, *268*, 1604. (b) Miller, R. D.; Burland, D. M.; Jurich, M.; Lee, V. Y.; Moylan, C. R.; Thackara, J. I.; Twieg, R. J.; Verbiest, T.; Volksen, W. *Macromolecules* **1995**, *28*, 4970. (c) Wang, J.-F.; Geng, L.; Lin, W.; Marks, T. J.; Wong, G. K. *Mater. Res. Soc. Symp. Proc.* **1995**, *392*, 85. (d) Geng, L.; Wang, J.-F.; Marks, T. J.; Line, W.; Zhou, H.; Lundquist, P. M.; Wong, G. K. *Mater. Res. Soc. Symp. Proc.* **1996**, *413*, 135.

(6) (a) Lundquist, P.; Jurich, M.; Burland, D. M.; Miller, R. D. Unpublished results. Data were acquired by heating the sample during contact poling and measuring the conductivity. (b) Yitzchaik, S.; DiBella, S.; Lundquist, P. M.; Wong, G. K.; Marks, T. J. *J. Am. Chem. Soc.* **1997**, *119*, 2995. (c) DiBella, S.; Lanza, G.; Fragala, I.; Yitzchaik, S.; Ratner, M. A.; Marks, T. J. *J. Am. Chem. Soc.* **1997**, *119*, 3003.

(7) Wu, X.; Wu, J.; Liu, Y.; Jen, A. K.-Y. *J. Am. Chem. Soc.* **1999**, *121*, 472.

(8) (a) Firestone, M. A.; Park, J.; Minami, N.; Ratner, M. A.; Marks, T. J.; Lin, W.; Wong, G. K. *Macromolecules* **1995**, *28*, 2247. (b) Firestone, M. A.; Ratner, M. A.; Marks, T. J.; Lin, W.; Wong, G. K. *Macromolecules* **1995**, *28*, 2260. (c) Firestone, M. A.; Ratner, M. A.; Marks, T. J. *Macromolecules* **1995**, *28*, 6296.

(9) Boyd, G. T. In *Polymers for Electronic and Photonic Applications*; Wong, C. P., Ed.; Academic Press: New York, 1993; p 467.

(10) Lipscomb, G. F.; Lytel, R. *Mol. Cryst. Liq. Cryst. Sci. Technol. B.; Nonlinear Opt.* **1992**, *3*, 41.

(11) (a) Park, J.; Marks, T. J.; Yang, J.; Wong, G. K. *Chem. Mater.* **1990**, *2*, 229. (b) Dai, D.-R.; Hubbard, M. A.; Li, D.; Park, J.; Ratner, M. A.; Marks, T. J.; Yang, J.; Wong, G. K. *ACS Symposium Series*; American Chemical Society: Washington, DC, 1991; Vol. 455, pp 226−249. (c) Jin, Y.; Carr, S. H.; Marks, T. J.; Lin, W.; Wong, G. K. *Chem. Mater.* **1992**, *4*, 963. (d) Hubbard, M. A.; Marks, T. J. *Chem. Mater.* **1992**, *4*, 965. (e) Crumpler, E. T.; Reznichenko, J. L.; Li, D.; Marks, T. J. *Chem. Mater.* **1995**, *7*, 596. (f) Yu, L.; Chan, W.; Dikshit, S.; Bao, Z.; Shi, Y.; Steier, W. H. *Appl. Phys. Lett.* **1992**, *60*, 1655. (g) Xu, C.; Wu, B.; Dalton, L. R.; Shi, Y.; Ranon, P. M.; Steier, W. H. *Macromolecules* **1992**, *25*, 6714. (h) Dalton, L. *Chem. Mater.* **1995**, *7*, 941.

(12) (a) Miller, R. D.; Burland, D. M.; Jurich, M.; Lee, V. Y.; Moylan, C. R.; Thackara, J. I.; Twieg, R. J.; Verbiest, T.; Volksen, W. *Macromolecules* **1995**, *28*, 4970. (b) Saadeh, H.; Gharavi, A.; Yu, D.; Yu, L. *Macromolecules* **1997**, *30*, 5403. (c) Shu, C.-F.; Shu, Y.-C.; Gong, Z.-H.; Peng, S.-M.; Lee, G.-H.; Jen, A. K. Y. *Chem. Mater.* **1998**, *10*, 3284.

(13) (a) Lin, J. T.; Hubbard, M. A.; Marks, T. J. *Chem. Mater.* **1992**, *4*, 1148. (b) Yu, D.; Gharavi, A.; Yu, L. *Macromolecules* **1995**, *28*, 784. (c) Yu, D.; Gharavi, A.; Yu, L. *J. Am. Chem. Soc.* **1995**, *117*, 11680. (d) Chen, T.-A.; Jen, A. K.-Y.; Cai, Y. *Macromolecules* **1996**, *29*, 535. (e) Woo, H.-Y.; Shim, H.-K.; Lee, K.-S.; Jeong, M.-Y.; Lim, T.-K. *Chem. Mater.* **1999**, *11*, 218.

(14) Moylan, C. R.; Twieg, R. J.; Lee, V. Y.; Swanson, S. A.; Betterton, K. M.; Miller, R. D. *J. Am. Chem. Soc.* **1993**, *115*, 12599.

TGA-7 thermogravimetric analyzer. Elemental analyses were performed by Galbraith Laboratories, Inc. All chromatography associated with product purification was performed by flash column techniques[15] using Merck Kieselgel 600 (230−400 mesh). Gel permeation chromatography (GPC) was carried out on a Waters chromatograph (four Waters Styragel HR columns HR1, HR2, HR4, and HR5E in series) connected to a Waters 410 differential refractometer and a Waters 996 Photodiode Array UV detector with THF as the carrier solvent. IR spectra were measured using an IBM IR/32 FT-IR. The UV−visible spectra were recorded on a Hewlett-Packard 8452 A diode array instrument. Film thicknesses were determined using a Tencor Alpha-Step 200 surface profilometer. All chemicals were obtained from Aldrich Chemical Co. and used as received except where indicated. The reagent 2-(1,3-dioxoisobenzofuran-5-ylcarbonyloxy)ethyl 1,3-dioxoisobenzofuran-5-carboxylate (TMEG-DA) was obtained from Chriskev Chemical Co. *N*-Methyl-2-pyrrolidone-d_9 was purchased from Cambridge Isotope Laboratories while 4-nitrostyrene was obtained from Polysciences, Inc. Commercial sodium hypochlorite (Clorox) was used for the preparation of *tert*-butyl hypochlorite which was freshly prepared as described elsewhere.[16] The preparation of tris(4-aminophenyl)amine was performed as described elsewhere.[17] THF was dried by distillation from Na−benzophenone.

Bis(4-trifluoroacetamidophenyl)(4-bromophenyl)-amine (3a). Trifluoroacetic anhydride (78.81 g, 0.375 mol) was added dropwise with stirring under argon to a solution of **2** (7.72 g, 21.8 mmol; see Supporting Information for synthesis) in 50 mL of dry THF and 10 mL of freshly distilled triethylamine in a 250 mL flask fitted with a magnetic stirring bar and water-cooled condenser. This solution was refluxed overnight, cooled, and then added to 300 mL of ethyl acetate. The organic phase was washed with water, 5% aqueous $NaHCO_3$ solution (2×), and dried over $MgSO_4$. The solution was then filtered, adsorbed onto silica gel, and chromatographed (20% ethyl acetate/hexane). Solvents were removed under reduced pressure and the resulting solids recrystallized from methanol/water to give **3a** as a colorless solid. Yield: 9.76 g (82%). Mp: 207 °C. ^{1}H NMR (DMSO-d_6): δ 11.23 (s, 2H, NH), 7.61 (d, 4H, J = 9 Hz, Ar), 7.40 (d, 2H, J = 9 Hz, Ar), 7.03 (d, 4H, J = 9 Hz, Ar), 6.88 (d, 2H, J = 9 Hz, Ar). ^{13}C NMR (DMSO-d_6): δ 154.24 (q, $^2J_{FC}$ = 37 Hz), 146.40, 143.92, 132.30, 131.87, 124.68, 124.50, 122.48, 115.84 (q, $^1J_{FC}$ = 289 Hz), 114.19. IR (KBr): 3276, 1709, 1543, 1512, 1491, 1331, 1290, 1248, 1166, 819, 736 cm^{-1}. UV (THF): λ_{max}, nm (ϵ) 322 (37 840). Anal. Calcd for $C_{22}H_{14}BrF_6N_3O_2$: C, 48.37; H, 2.58; N, 7.69. Found: C, 48.39; H, 2.60; N, 7.57.

Bis[4-((*tert*-butoxy)carbonylamino)phenyl](4-bromophenyl)amine (3b). In a 500 mL flask equipped with a magnetic stirring bar, water-cooled condenser, and argon inlet was placed **2** (7.97 g, 22.5 mmol), dry THF (85 mL). and freshly distilled triethylamine (15 mL). Di-*tert*-butyl dicarbonate (*t*-BOC anhydride; 14.00 g, 64.1 mmol) was added with stirring, and the solution heated at reflux overnight. The solution was next adsorbed onto silica gel and chromatographed (20% ethyl acetate/hexane) to give **3b** as a colorless solid which was sufficiently pure for subsequent reactions. Yield: 9.70 g (78%). Mp: 241 °C (dec). ^{1}H NMR (DMSO-d_6): δ 9.33 (s, 2H, NH), 7.38 (d, 4H, J = 9 Hz, Ar), 7.31 (d, 2H, J = 9 Hz, Ar), 6.93 (d, 4H, J = 9 Hz, Ar), 6.72 (d, 2H, J = 9 Hz, Ar), 1.45 (s, 18H, CH_3). ^{13}C NMR (DMSO-d_6): δ 152.82, 147.37, 140.89, 135.68, 131.80, 125.43, 121.91, 119.55, 111.69, 78.96, 28.13. IR (KBr): 3320, 2978, 1700, 1515, 1488, 1314, 1243, 1172, 1063, 835 cm^{-1}. UV (THF): λ_{max}, nm (ϵ) 310 (32 550). Anal. Calcd for $C_{28}H_{32}BrN_3O_4$: C, 60.65; H, 5.82; N, 7.58. Found: C, 60.71; H, 5.95; N, 7.61.

Bis(4-trifluoroacetamidophenyl)(4-nitrophenyl)-amine (5a). Trifluoroacetic anhydride (78.81 g, 0.375 mol) was added dropwise with stirring to a solution of **4** (12.98 g, 40.5 mmol; see Supporting Information for synthesis) in 150 mL of dry THF and 30 mL of freshly distilled triethylamine under argon in a 500 mL flask fitted with a magnetic stirring bar and water-cooled condenser. This solution was refluxed overnight, cooled, and 300 mL of ethyl acetate added. The organic solution was washed with water, 5% aqueous $NaHCO_3$ solution (2×), and dried over $MgSO_4$. After filtering, the solvent was removed under reduced pressure, and the resulting solids recrystallized from acetone to afford **5a** as red needles. Yield: 19.0 g (91%). Mp: 221 °C. ^{1}H NMR (DMSO-d_6): δ 11.37 (d, 2H, NH), 8.06 (d, 2H, J = 9 Hz, Ar), 7.73 (d, 4H, J = 9 Hz, Ar), 7.27 (d, 4H, J = 9 Hz, Ar), 6.84 (d, 2H, J = 9 Hz, Ar). ^{13}C NMR (DMSO-d_6): δ 154.44 (q, $^2J_{FC}$ = 36.7 Hz), 153.02, 141.99, 139.30, 134.16, 127.19, 125.67, 122.68, 118.06, 115.77 (q, $^1J_{FC}$ = 288.6 Hz). IR (KBr): 3550−3050, 1700, 1591, 1547, 1509, 1314, 1248, 1150, 1112, 840 cm^{-1}. UV (THF): λ_{max}, nm (ϵ) 400 (19 710). Anal. Calcd for $C_{22}H_{14}F_6N_4O_4$: C, 51.57; H, 2.75; N, 10.93. Found: C, 51.24; H, 2.88; N, 10.83.

Bis[4-((*tert*-butoxy)carbonylamino)phenyl](4-nitrophenyl)amine (5b). In a 500 mL flask equipped with a magnetic stirring bar, water-cooled condenser, and argon inlet was placed **4** (6.53 g, 20.4 mmol), dry THF (85 mL), and freshly distilled triethylamine (15 mL). Di-*tert*-butyl dicarbonate (*t*-BOC anhydride; 14.00 g, 0.0641 mol) was added and the solution heated at reflux overnight. The solution was then adsorbed onto silica gel, chromatographed (33% ethyl acetate/hexane), and recrystallized from toluene to afford **5b** as a colorless solid. Yield: 4.92 g (46%). Mp: 230 °C. ^{1}H NMR (DMSO-d_6): δ 9.49 (s, 2H, NH), 8.00 (d, 2H, J = 9 Hz, Ar), 7.51 (d, 4H, J = 9 Hz, Ar), 7.14 (d, 4H, J = 9 Hz, Ar), 6.67 (d, 2H, J = 9 Hz, Ar), 1.45 (s, 18H, CH_3). ^{13}C NMR (DMSO-d_6): δ 153.79, 152.76, 138.70, 138.08, 137.84, 127.41, 125.65, 119.61, 115.26, 79.20, 28.08. IR (KBr): 3348, 2981, 2940, 1728, 1588, 1518, 1320, 1233, 1169, 1117, 1058, 843 cm^{-1}. UV (THF): λ_{max}, nm (ϵ) 406 (19 390). Anal. Calcd for $C_{28}H_{32}N_4O_6$: C, 64.60; H, 6.20; N, 10.76. Found: C, 64.88; H, 6.09; N, 10.58.

(4-Aminophenyl)[bis(4-trifluoroacetamidophenyl)]-amine (6a). A solution of **5a** (10.18 g, 19.9 mmol) in 250 mL of ethyl acetate was hydrogenated (40 psi) over 10% Pd/C (1.10 g) by shaking in a Parr hydrogenator for 2 h. The mixture was then filtered through Celite, the solvent removed from the filtrate under reduced pressure, and the resulting solid recrystallized from benzene to afford **6a** as a colorless solid. Yield: 9.06 g (95%). Mp: 345 °C (dec). ^{1}H NMR (DMSO-d_6): δ 11.13 (s, 2H, NHCO), 7.50 (d, 4H, J = 9 Hz, Ar), 6.91 (d, 4H, J = 9 Hz, Ar), 6.80 (d, 2H, J = 9 Hz, Ar), 6.57 (d, 2H, J = 9 Hz, Ar), 5.11 (s, 2H, NH_2). ^{13}C NMR (DMSO-d_6): δ 154.08 (q, $^2J_{FC}$ = 36.7 Hz), 146.47, 145.31, 134.79, 129.72, 127.94, 122.22, 121.58, 115.91 (q, $^1J_{FC}$ = 288.8 Hz), 115.04. IR (KBr): 3650−3150, 1705, 1547, 1509, 1259, 1161, 835 cm^{-1}. UV (THF): λ_{max}, nm (ϵ) 326 (26 670). Anal. Calcd for $C_{22}H_{16}F_6N_4O_2$: C, 54.78; H, 3.34; N, 11.61. Found: C, 54.36; H, 3.54; N, 11.49.

Bis[4-((*tert*-butoxy)carbonylamino)phenyl](4-aminophenyl)amine (6b). Using the same procedure as described for **6a**, reduction of **5b** (10.13 g, 19.5 mmol) followed by precipitation with water gave **6b** as a colorless solid which was sufficiently pure for subsequent reactions. Yield: 9.10 g (95%). Mp: 244 °C. ^{1}H NMR (DMSO-d_6): δ 9.14 (s, 2H, NH), 7.26 (d, 4H, J = 9 Hz, Ar), 6.76 (d, 4H, J = 9 Hz, Ar), 6.72 (d, 2H, J = 9 Hz, Ar), 6.52 (d, 2H, J = 9 Hz, Ar), 4.96 (s, 2H, NH_2), 1.44 (s, 18H, CH_3). ^{13}C NMR (DMSO-d_6): δ 152.90, 145.34, 143.02, 136.16, 133.11, 126.82, 121.99, 114.91, 78.66, 28.15. IR (KBr): 3365, 2975, 2934, 1705, 1606, 1518, 1379, 1274, 1233, 1169, 1058, 843 cm^{-1}. UV (THF): λ_{max}, nm (ϵ) 314 (30 010). Anal. Calcd for $C_{28}H_{34}N_4O_4$: C, 68.55; H, 6.99; N, 11.42. Found: C, 68.49; H, 7.10; N, 11.13.

2-Vinyl-6-nitrobenzothiazole (8). To a 250 mL flask equipped with a water cooled condenser, magnetic stirring bar, and argon inlet were added **7** (4.00 g, 13.1 mol; see Supporting Information for synthesis), dichlorobis(triphenylphosphine)-palladium(II) (0.1943 g, 0.277 mmol), and 1,2-dichloroethane (100 mL). Vinyltributyl tin (4.98 g, 15.7 mmol) was then added and the solution heated with stirring at 80 °C for 5 h. The crude product was then adsorbed onto silica gel, chromatographed (10% ethyl acetate/hexane), and recrystallized from

(15) Still, W. C.; Kahn, M.; Mitra, A. *J. Org. Chem.* **1978**, *43*, 2923.
(16) Mintz, M. J.; Walling, C. *Org. Synth., Collect. Vol. V* **1973**, 183.
(17) Haeussermann, C. *Chem. Ber.* **1906**, *39*, 2763.

2-propanol to give **8** as light-orange needles. Yield: 1.89 g (70%). Mp: 159 °C (dec). ^{1}H NMR (DMSO-d_6): δ 9.15 (s, 1H, Ar), 8.31 (d, 1H, J = 9 Hz, Ar), 8.13 (d, 1H, J = 9 Hz, Ar), 7.16 (q, 1H, J = 11 Hz, vinyl), 6.41 (d, 1H, J = 17 Hz, vinyl), 5.99 (d, 1H, J = 11 Hz, vinyl). ^{13}C NMR (DMSO-d_6): δ 172.75, 156.93, 144.58, 134.69, 130.58, 126.65, 123.19, 121.79, 119.43. IR (KBr): 3095, 1522, 1347, 943, 830, 763 cm^{-1}. UV (THF): λ_{max}, nm (ϵ) 314 (17 840). Anal. Calcd for $C_9H_6N_2O_2S$: C, 52.42; H, 2.93; N, 13.58. Found: C, 52.14; H, 2.75; N, 13.48.

2-(4-(Hydroxylamino)phenyl)-2-phenyl-1,1-dicyanoethylene (11). Into a 125 mL three-neck flask equipped with an overhead stirrer were placed 40 mL of THF and 6.01 g (21.8 mmol) **10** (see Supporting Information for synthesis) under argon. Sodium hypophosphite nonahydrate (5.89 g, 55.6 mmol) was dissolved in 30 mL of distilled water and added to the THF solution. The solution was next cooled in an ice/water bath, 10% Pd/C (0.60 g) was added, and the solution was stirred vigorously while monitoring the reaction progress by TLC (5% ethyl acetate/dichloromethane). Upon consumption of the starting material (45 min), the mixture was filtered through Celite, 100 mL of ethyl acetate added, and the organic phase was washed with distilled water (3×). The organic layer was then separated, dried over $MgSO_4$, filtered, adsorbed onto silica gel, and chromatographed (gradient elution: 0%, 5%, 10% ethyl acetate/methylene chloride.) The bright-orange product (**11**) was used without further purification. Yield: 5.19 g (91%). Mp: 169 °C (dec). ^{1}H NMR (DMSO-d_6): δ 9.49 (s, 1H, *NH*OH), 8.95 (s, 1H, NH*OH*), 7.57 (m, 3H, Ar), 7.43 (d, 2H, J = 7 Hz, Ar), 7.32 (d, 2H, J = 9 Hz, Ar), 6.82 (d, 2H, J = 9 Hz, Ar). ^{13}C NMR (DMSO-d_6): δ 173.40, 155.93, 136.68, 132.87, 131.90, 130.38, 128.67, 124.02, 115.82, 115.46, 110.62, 74.44. IR (KBr): 3500−3350, 3302, 2231, 1605, 1513, 1347, 1181, 840, 778, 705, 607 cm^{-1}. UV (THF): λ_{max}, nm (ϵ) 380 (26 380). EI MS: m/z 261 (M^+). Anal. Calcd for $C_{16}H_{11}N_3O$: C, 73.55; H, 4.24; N, 16.08. Found: C, 73.75; H, 4.27; N, 15.78.

2-(4-Nitrosophenyl)-2-phenyl-1,1-dicyanoethylene (12). In a three-necked 1 L flask fitted with a gas inlet valve, thermometer, and magnetic stirring bar, 1.07 g (4.11 mmol) of **11** was dissolved in 500 mL of diethyl ether under argon and cooled to −78 °C. The solution was stirred rapidly and *tert*-butyl hypochlorite (0.446 g, 4.11 mmol) added in a single portion. The stirring was continued for an additional 5 min. The cooling bath was next removed, and the solution allowed to warm to −20 °C. The solvent was then removed under reduced pressure at 0 °C, and the residual solids were further dried under high vacuum at room temperature. The product (**12**) was sufficiently pure as isolated for subsequent derivatization. Yield: 1.01 g (95%). Mp: 105 °C. ^{1}H NMR (DMSO-d_6): δ 8.10 (d, 2H, J = 7 Hz, Ar), 7.87 (d, 2H, J = 7 Hz, Ar), 7.57 (m, 5H, Ar). ^{13}C NMR (DMSO-d_6): δ 171.82, 163.92, 142.70, 135.15, 132.87, 131.92, 130.11, 129.05, 120.67, 113.80, 113.70, 84.54. IR (KBr): 2231, 1159, 1269, 716 cm^{-1}. UV (THF): λ_{max}, nm (ϵ) 294 (18 157). EI MS: m/z 259 (M^+). Anal. Calcd for $C_{16}H_9N_3O$: C, 74.12; H, 3.50; N, 16.21. Found: C, 74.04; H, 3.88; N, 15.95.

Bis(4-trifluoroacetamidophenyl)[4-(2-(4-nitrophenyl)-vinyl)phenyl]amine (13a). In a 250 mL flask equipped with water-cooled condenser and magnetic stirring bar were placed **3a** (12.13 g, 22.2 mmol), 4-nitrostyrene (4.85 g, 32.5 mol), palladium(II) acetate (0.162 g, 0.723 mmol), and tris-*o*-tolylphosphine (2.96 g, 9.72 mmol) under argon. Freshly distilled triethylamine (50 mL) and DMF (50 mL) were added, and the reaction mixture was heated at reflux for 4 days. The solvent was removed under reduced pressure and the residue dissolved in ethyl acetate (200 mL) and washed repeatedly with water (5×). The organic layer was then dried over magnesium sulfate, filtered, adsorbed onto silica gel, and chromatographed with 20% acetone/hexane. Recrystallization from toluene or benzene gave **13a** as a red solid. Yield: 6.82 g (50%). Mp: 190 °C. ^{1}H NMR (DMSO-d_6): δ 11.25 (s, 2H, NH), 8.19 (d, 2H, J = 9 Hz, Ar), 7.80 (d, 2H, J = 9 Hz, Ar), 7.63 (d, 4H, J = 9 Hz, Ar), 7.57 (d, 2H, J = 9 Hz, Ar), 7.47 (d, 1H, J = 16 Hz, stilbene), 7.25 (d, 1H, J = 16 Hz, stilbene), 7.08 (d, 4H, J = 9 Hz, Ar), 6.96 (d, 2H, J = 9 Hz, Ar). ^{13}C NMR (DMSO-d_6): δ 154.26 (q, $^2J_{FC}$ = 37 Hz), 147.40, 145.84, 144.41, 143.86, 132.81, 132.00, 130.38, 128.46, 126.95, 124.83, 124.58, 124.04, 122.46, 122.25, 115.85 (q, $^1J_{FC}$ = 288 Hz). IR (KBr): 3307, 3074, 1698, 1590, 1543, 1506, 1347, 1284, 1243, 1155, 834, 736, 524 cm^{-1}. UV (THF): λ_{max}, nm (ϵ) 430 (25 990). Anal. Calcd for $C_{30}H_{20}F_6N_4O_4$: C, 58.64; H, 3.28; N, 9.12. Found: C, 58.48.17; H, 3.33; N, 8.89.

Bis[4-((*tert*-butoxy)carbonylamino)phenyl][4-(2-(4-nitrophenyl)vinyl)phenyl]amine (13b). In a 250 mL flask equipped with water cooled condenser, magnetic stirring bar and argon inlet were placed **3b** (11.73 g, 21.2 mmol), 4-nitrostyrene (4.80 g, 32.2 mmol), palladium(II) acetate (0.197 g, 0.878 mmol), and tris-*o*-tolylphosphine (3.43 g, 11.27 mmol). Freshly distilled triethylamine (50 mL) and DMF (50 mL) were added, and the solution was heated at reflux for 4 days. The solvent was then removed under reduced pressure, and the residue was dissolved in ethyl acetate (200 mL) and washed repeatedly with water (5×). The organic layer was dried over magnesium sulfate, filtered, adsorbed onto silica gel, and chromatographed with 25% ethyl acetate/hexane to give **13b** as a red solid which was sufficiently pure for subsequent reactions. Yield: 5.66 g (43%). Mp: 160 °C. ^{1}H NMR (DMSO-d_6): δ 9.35 (s, 2H, NH), 8.18 (d, 2H, J = 9 Hz, Ar), 7.78 (d, 2H, J = 9 Hz, Ar), 7.45 (m, 7H, Ar), 7.18 (d, 1H, J = 16 Hz, stilbene vinyl proton), 6.98 (d, 4H, J = 9 Hz, Ar), 6.79 (d, 2H, J = 9 Hz, Ar), 1.46 (s, 18H, *tert*-butyl CH3). ^{13}C NMR (DMSO-d_6): δ 152.87, 148.42, 145.58, 144.62, 140.78, 135.77, 133.09, 128.28, 126.74, 125.74, 124.02, 123.39, 119.56, 79.08, 28.09. IR (KBr): 3421, 2981, 2929, 1688, 1590, 1507, 1367, 1341, 1274, 1233, 1160, 1109, 1057, 840, 534 cm^{-1}. UV (THF): λ_{max}, nm (ϵ) 448 (25 830). Anal. Calcd for $C_{36}H_{38}N_4O_6$: C, 69.44; H, 6.15; N, 9.00. Found: C, 69.57; H, 5.98; N, 9.34.

Bis(4-aminophenyl)[4-(2-(4-nitrophenyl)vinyl)phenyl]-amine (14). *From **13a***. To a solution of **13a** (4.50 g, 7.32 mmol) in freshly distilled THF (80 mL) under argon was added dropwise with stirring potassium carbonate (4.12 g, 29.81 mmol) dissolved in argon-degassed water (45 mL). The solution was then heated with stirring at 45 °C for 48 h. The solvent was removed under reduced pressure, and the residue was dissolved in ethyl acetate and washed with water (3×). The organic layer was dried over sodium sulfate, filtered, adsorbed onto silica gel, and purified by flash chromatography (gradient: 0%, 5%, 10%, 25%, 33%, 50% ethyl acetate/diethyl ether.) Recrystallization from toluene/hexane gave **14** as a dark-red solid. Yield: 2.93 g (95%). Mp: 193 °C.

*From **13b***. In a 1 L flask under argon **13b** (3.94 g, 6.33 mmol) was dissolved in 250 mL of ethyl acetate. A solution of concentrated HCl (100 mL) and ethyl acetate (200 mL) was prepared, added dropwise with stirring, and the entire solution stirred overnight. The solution was then extracted with 5% aqueous sodium carbonate solution (3×) and water (2×), dried over magnesium sulfate, filtered, and chromatographed (gradient: 0%, 5%, 10%, 25%, 33%, 50% ethyl acetate/diethyl ether.) Recrystallization from toluene/hexane gave **14** as a dark-red solid. Yield: 2.55 g (95%). Mp: 195 °C. ^{1}H NMR (DMSO-d_6): δ 8.15 (d, 2H, J = 9 Hz, Ar), 7.73 (d, 2H, J = 9 Hz, Ar), 7.37 (m, 3H, Ar), 7.06 (d, 1H, J = 16 Hz, stilbene vinyl proton), 6.84 (d, 4H, J = 9 Hz, Ar), 6.56 (m, 6H, Ar), 5.05 (s, 4H, NH2). ^{13}C NMR (DMSO-d_6): δ 150.26, 146.16, 145.25, 145.06, 135.03, 133.67, 128.14, 127.64, 126.42, 125.49, 124.04, 121.67, 115.83, 114.79. IR (KBr): 3436, 3369, 3038, 1626, 1579, 1507, 1336, 1269, 1176, 1109, 959, 829, 571, 524 cm^{-1}. UV (THF): λ_{max}, nm (ϵ): 474 (26 200). Anal. Calcd for $C_{26}H_{22}N_4O_2$: C, 73.92; H, 5.25; N, 13.26. Found: C, 73.87; H, 5.36; N, 13.59.

Bis(4-trifluoroacetamidophenyl)[4-(2-(6-nitrobenzothiazol-2-yl)vinyl)phenyl]amine (15). In a 250 mL flask equipped with a water-cooled condenser and magnetic stirring bar under argon were placed **3a** (8.20 g, 15.0 mmol), **8** (2.75 g, 13.3 mol), palladium(II) acetate (0.0813 g, 0.362 mmol), and tris-*o*-tolylphosphine (2.0442 g, 6.72 mmol). Freshly distilled triethylamine (50 mL) and freshly distilled DMF (40 mL) were then added, and the solution was heated at reflux with stirring for 4 days. The solvent was then removed under reduced pressure, and the residue was dissolved in ethyl acetate (200 mL) and washed repeatedly with water (5×). The organic layer was dried over magnesium sulfate, filtered, adsorbed onto

silica gel, and chromatographed with 33% ethyl acetate/hexane. Recrystallization from 2-propanol gave **15** as a red-orange solid. Yield: 4.48 g (50%). Mp: 230 °C. ^{1}H NMR (DMSO-d_6): δ 11.23 (s, 2H, NH), 9.02 (s, 1H, Ar), 8.21 (d, 1H, J = 9 Hz, Ar), 7.98 (d, 1H, J = 9 Hz, Ar), 7.61 (m, 7H, Ar), 7.42 (d, 1H, J = 16 Hz, stilbene vinyl proton), 7.06 (d, 4H, J = 9 Hz, Ar), 6.86 (d, 2H, J = 9 Hz, Ar). ^{13}C NMR (DMSO-d_6): δ 173.20, 157.52, 154.28 (q, $^2J_{FC}$ = 37 Hz), 148.70, 143.98, 143.42, 139.38, 134.66, 133.40, 132.51, 129.57, 128.88, 128.17, 125.46, 122.39, 121.84, 121.03, 119.09, 118.88, 115.83 (q, $^1J_{FC}$ = 288 Hz). IR (KBr): 3441, 3297, 1709, 1595, 1538, 1512, 1347, 1279, 1248, 1181, 819, 747, 519 cm^{-1}. UV (THF): λ_{max}, nm (ϵ): 448 (40 860). Anal. Calcd for $C_{31}H_{19}F_6N_5O_4S$: C, 55.44; H, 2.85; N, 10.43. Found: C, 55.17; H, 2.46; N, 10.67.

Bis(4-aminophenyl)[4-(2-(6-nitrobenzothiazol-2-yl)-vinyl)phenyl]amine (16). To a solution of **15** (3.53 g, 5.26 mmol) in freshly distilled THF (60 mL) under argon was added dropwise K_2CO_3 (2.94 g, 21.27 mmol) dissolved in argon-degassed water (30 mL). The solution was heated with stirring at 45 °C for 48 h. The solvent was then removed under reduced pressure, and the residue was dissolved in ethyl acetate (200 mL) and washed with water (3×). The organic layer was next dried over sodium sulfate, filtered, adsorbed onto silica gel, and purified by flash chromatography (gradient: 0%, 5%, 10%, 25%, 33%, 50% ethyl acetate/diethyl ether). Recrystallization from ethyl acetate/2-propanol gave **16** as a dark-red solid. Yield: 2.39 g (95%). Mp: 263 °C. ^{1}H NMR (DMSO-d_6): δ 9.05 (s, 1H, Ar), 8.26 (d, 1H, J = 9 Hz, Ar), 7.99 (d, 1H, J = 9 Hz, Ar), 7.62 (d, 1H, J = 16 Hz, stilbene), 7.49 (d, 2H, J = 9 Hz, Ar), 7.32 (d, 1H, J = 16 Hz, stilbene), 6.87 (d, 4H, J = 9 Hz, Ar), 6.55 (m, 6H, Ar), 5.11 (s, 4H, NH_2). ^{13}C NMR (DMSO-d_6): δ 173.75, 157.70, 151.47, 146.37, 143.69, 140.43, 134.54, 134.41, 129.48, 127.85, 123.64, 121.89, 118.85, 116.01, 115.26, 114.84. IR (KBr): 3431, 3364, 1590, 1512, 1476, 1336, 1274, 1186, 814 cm^{-1}. UV (THF): λ_{max}, nm (ϵ) 488 (36 641). Anal. Calcd for $C_{27}H_{21}N_5O_2S$: C, 67.62; H, 4.41; N, 14.60. Found: C, 67.26; H, 4.29; N, 14.60.

2-[4-((4-(Bis(4-((*tert*-butoxy)carbonylamino)phenyl)-amino)phenyl)diazenyl)phenyl]-2-phenyl-1,1-dicyano-ethylene (17). To a solution of **12** (1.75 g, 6.75 mmol) in THF (50 mL) was added glacial acetic acid (25 mL) followed by **6b** (3.35 g, 6.83 mmol), and the resulting solution was stirred overnight. The solvent was removed under reduced pressure, and the residual solids were redissolved in ethyl acetate (200 mL) and extracted with water (3×). The organic layer was dried over magnesium sulfate, filtered, adsorbed onto silica gel, and purified by chromatography eluting with 33% ethyl acetate/hexane. This gave **17** as a dark-purple solid which was sufficiently pure for subsequent reactions. Yield: 2.99 g (58%). Mp: 246 °C. ^{1}H NMR (DMSO-d_6): δ 9.44 (s, 2H, NH), 7.89 (d, 2H, J = 9 Hz, Ar), 7.76 (d, 2H, J = 9 Hz, Ar), 7.55 (m, 11H, Ar), 7.10 (d, 4H, J = 9 Hz, Ar), 6.83 (d, 2H, J = 9 Hz, Ar), 1.46 (s, 18H, CH_3). ^{13}C NMR (DMSO-d_6): δ 173.09, 154.42, 152.79, 151.85, 145.10, 139.85, 137.07, 136.83, 135.86, 132.61, 131.75, 130.29, 128.92, 126.90, 125.04, 122.15, 119.56, 117.45, 114.28, 82.05, 79.12, 28.11. IR (KBr): 3390, 2976, 2226, 1729, 1594, 1512, 1310, 1166, 1140, 1057, 840 cm^{-1}. UV (THF): λ_{max}, nm (ϵ) 510 (29 540). Anal. Calcd for $C_{44}H_{41}N_7O_4$: C, 72.21; H, 5.65; N, 13.40. Found: C, 72.37; H, 5.39; N, 13.63.

2-[4-((4-(Bis(4-aminophenyl)amino)phenyl)diazenyl)-phenyl]-2-phenyl-1,1-dicyanoethylene (18). In a 1 L flask under argon **17** (3.12 g, 4.26 mmol) was dissolved in 200 mL of ethyl acetate. A solution of concentrated HCl (100 mL) and ethyl acetate (200 mL) was prepared, added dropwise with stirring, and the solution stirred overnight. The solution was then extracted with 5% aqueous sodium carbonate solution (3×) and water (2×), dried over magnesium sulfate, filtered, and chromatographed eluting with 70% ethyl acetate/hexane. Recrystallization from 1-propanol gave **18** as a deeply colored solid. Yield: 2.11 g (93%). Mp: 293 °C (dec). ^{1}H NMR (DMSO-d_6): δ 7.85 (d, 2H, J = 9 Hz, Ar), 7.58 (m, 9H, Ar), 6.93 (d, 4H, J = 9 Hz, Ar), 6.65 (d, 2H, J = 9 Hz, Ar), 6.58 (d, 4H, J = 9 Hz, Ar), 5.18 (s, 4H, NH_2). ^{13}C NMR (DMSO-d_6): δ 173.16, 154.70, 153.37, 147.06, 143.86, 136.24, 135.92, 133.89, 132.58, 131.76, 130.31, 128.91, 127.97, 125.20, 121.93, 114.92, 114.79, 114.36, 81.71. IR (KBr): 3447, 3379, 2226, 1595, 1512, 1497, 1316, 1140, 829 cm^{-1}. UV (THF): λ_{max}, nm (ϵ) 532 (24 340). Anal. Calcd for $C_{34}H_{25}N_7$: C, 76.82; H, 4.74; N, 18.44. Found: C, 76.62; H, 4.61; N, 18.14.

2-[4-((4-(Bis(4-trifluoroacetamidophenyl)amino)-phenyl)diazenyl)phenyl]-2-phenyl-1,1-dicyanoethylene (19). To a solution of **12** (1.75 g, 6.75 mmol) in THF (50 mL) was added glacial acetic acid (25 mL) followed by **6a** (3.29 g, 6.82 mmol), and the reaction mixture was stirred overnight. The solvent was then removed under reduced pressure, and the residual solids were redissolved in ethyl acetate (200 mL) and extracted with water (3×). The organic layer was dried over magnesium sulfate, filtered, adsorbed onto silica gel, and chromatographed by eluting with 33% ethyl acetate/hexane. This gave **19** as a dark-red solid which was sufficiently pure for subsequent reactions. Yield: 3.11 g (64%). Mp: 158 °C. ^{1}H NMR (DMSO-d_6): δ 11.33 (s, 2H, NH), 7.92 (d, 2H, J = 9 Hz, Ar), 7.83 (d, 2H, J = 9 Hz, Ar), 7.63 (m, 12H, Ar), 7.21 (d, 4H, J = 9 Hz, Ar), 7.00 (d, 2H, J = 9 Hz, Ar). ^{13}C NMR (DMSO-d_6): δ 173.03, 154.37 (q, $^2J_{FC}$ = 37 Hz), 154.23, 150.90, 146.17, 142.92, 137.26, 135.82, 133.25, 132.64, 131.75, 130.28, 128.93, 126.32, 124.97, 122.58, 122.30, 119.88, 115.81 (q, $^1J_{FC}$ = 288 Hz), 114.23, 82.29. IR (KBr): 3431, 3276, 3131, 3079, 2226, 1714, 1600, 1512, 1295, 1248, 1160, 834 cm^{-1}. UV (THF): λ_{max}, nm (ϵ) 486 (30 350). Anal. Calcd for $C_{38}H_{23}F_6N_7O_2$: C, 63.07; H, 3.20; N, 13.55. Found: C, 62.88; H, 2.99; N, 13.69.

2-[4-((4-(Diphenylamino)phenyl)diazenyl)phenyl]-2-phenyl-1,1-dicyanoethylene (24). To a solution of **12** (1.49 g, 5.75 mmol) in THF (50 mL) was added glacial acetic acid (25 mL) followed by 4-aminotriphenylamine (1.51 g, 5.80 mmol), and the resulting solution was stirred overnight. The solvent was removed under reduced pressure, and the residual solids were redissolved in ethyl acetate (200 mL) and extracted with water (3×). The organic layer was dried over magnesium sulfate, filtered, adsorbed onto silica gel, and purified by flash chromatography eluting with 33% ethyl acetate/hexane. Recrystallization from methylcyclohexane gave **24** as a darkly colored solid. Yield: 1.21 g (42%). Mp: 225 °C. ^{1}H NMR (DMSO-d_6): δ 7.91 (d, 2H, J = 9 Hz, Ar), 7.82 (d, 2H, J = 9 Hz, Ar), 7.66−7.53 (cm, 7H, Ar), 7.43−7.37 (cm, 4H, Ar), 7.23−7.17 (cm, 6H, Ar), 6.96 (d, 2H, J = 9 Hz, Ar). ^{13}C NMR (DMSO-d_6): δ 173.09, 154.31, 151.29, 146.00, 145.87, 137.19, 135.84, 132.61, 131.70, 130.24, 129.97, 128.93, 126.05, 125.16, 124.90, 122.25, 119.60, 114.20, 82.29. IR (KBr): 2231, 1594, 1543, 1502, 1445, 1424, 1398, 1331, 1290, 1140, 850, 767, 705, 514 cm^{-1}. UV (THF): λ_{max}, nm (ϵ) 480 (34 990). Anal. Calcd for $C_{34}H_{23}N_5$: C, 81.42; H, 4.62; N, 13.96. Found: C, 81.65; H, 4.73; N, 14.28.

General Procedure for Preparation of Chromophore-Embedded Polyimide Derivatives. In a glovebox, 1.0 g of the chromophore diamine was dissolved in 7.0 mL of dry NMP. An equimolar amount of the dianhydride was added and washed into the flask with additional NMP such that the total weight of monomers represented ∼15% of the weight of the total solution. This polymerization mixture was stirred overnight in the glovebox, producing a viscous, deep-red solution. After the reaction mixture was removed from the glovebox, imidization was initiated by the addition of 4.0 equiv each of pyridine and acetic anhydride. The mixture was stirred for an additional 2 days under argon at ambient temperature. The homogeneous polymer solution was then poured into ∼400 mL of 75% methanol/water while agitating with a high-speed blender to ensure good mixing and particle formation. The solids were collected, redissolved in a minimum amount of NMP, and reprecipitated with methanol in the same manner. Filtration and drying under high vacuum yielded the desired polymeric products in high yield (>94%). In this manner, the six polymers shown in Figure 4 were prepared.

6F-DCVPh-Azo (29). This material was prepared from **18** and **27** and obtained as a dark-red solid in 96% yield. ^{1}H NMR (NMP-d_9): δ 7.62 (d, 2H, J = 8 Hz, Ar), 7.49−7.31 (m, 6H, Ar), 7.19−6.79 (m, 17H, Ar), 6.59 (d, 2H, J = 8 Hz, Ar). IR (film, NaCl): 3053, 2919, 2221, 1802, 1734, 1610, 1512, 1445, 1388, 1331, 1305, 1259, 1212, 1191, 1140, 1103, 984, 850, 725

cm^{-1}. UV (film): λ_{max}, nm (α_A) 474 (6.63 μm^{-1}). T_g (DSC): 313 °C. T_d (TGA): 475 °C (5wt % loss). GPC (polystyrene equivalent): M_n = 161 000, PDI = 2.10. Anal. Calcd for $C_{53}H_{27}F_6N_7O_4$: C, 67.73; H, 2.90; N, 10.43. Found: C, 67.82; H, 2.55; N, 10.15.

6F-NBT-Stil (30). This material was prepared from **16** and **27** and obtained as a dark-orange solid in 95% yield. ^{1}H NMR (NMP-d_9): δ 8.61 (s, 1H, Ar), 7.76 (d, 1H, J = 8 Hz, Ar), 7.63 (d, 2H, J = 8 Hz, Ar), 7.56−7.48 (m, 3H, Ar), 7.31−7.26 (m, 5H, Ar), 7.11−7.03 (m, 5H, Ar), 6.75 (d, 4H, J = 8 Hz, Ar), 6.53 (d, 2H, J = 8 H, Ar). IR (film, NaCl): 3488, 3059, 2991, 1786, 1719, 1590, 1507, 1466, 1440, 1378, 1336, 1279, 1259, 1217, 1191, 1150, 1098, 959, 824, 716 cm^{-1}. UV (film): λ_{max}, nm (α_A) 440 (11.14 μm^{-1}). T_g (DSC): not observed. T_d (TGA): 415 °C (5 wt % loss). GPC (polystyrene equivalent): M_n = 69 900, PDI = 1.79. Anal. Calcd for $C_{46}H_{23}F_6N_5O_6S$: C, 62.24; H, 2.61; N, 7.89. Found: C, 62.60; H, 2.88; N, 8.04.

6F-NO2-Stil (31). This material was prepared from **14** and **27** and obtained as an orange solid in 96% yield. ^{1}H NMR (NMP-d_9): δ 7.66−7.61 (m, 4H, Ar), 7.49 (d, 2H, J = 8 Hz, Ar), 7.37−7.30 (m, 4H, Ar), 7.17 (d, 2H, J = 8 Hz, Ar), 7.11−6.84 (m, 5H, Ar), 6.68 (d, 4H, J = 8 Hz, Ar), 6.55 (d, 2H, J = 8 Hz, Ar). IR (film, NaCl): 3483, 3028, 1781, 1724, 1590, 1507, 1367, 1341, 1321, 1259, 1217, 1202, 1145, 1109, 969, 829, 716, 529 cm^{-1}. UV (film): λ_{max}, nm (α_A) 418 (8.40 μm^{-1}). T_g (DSC): 312 °C. T_d (TGA): 420 °C (5wt % loss). GPC (polystyrene equivalent): M_n = 17 300, PDI = 2.35. Anal. Calcd for $C_{45}H_{24}F_6N_4O_6$: C, 65.07; H, 2.91; N, 6.75. Found: C, 65.19; H, 3.16; N, 6.99.

TMEG-DCVPh-Azo (32). This material was prepared from **18** and **28** and obtained as a dark-red solid in 97% yield. ^{1}H NMR (NMP-d_9): δ 7.93 (d, 2H, J = 8 Hz, Ar), 7.78 (s, 2H, Ar), 7.55 (d, 2H, J = 8 Hz, Ar), 7.39−7.32 (m, 5H, Ar), 7.17−6.93 (m, 10H, Ar), 6.78 (d, 4H, J = 8 Hz, Ar), 6.57 (d, 2H, J = 8 Hz, Ar), 4.27 (s, 4H, CH_2). IR (film, NaCl): 3488, 3043, 3002, 2231, 1791, 1724, 1595, 1517, 1444, 1429, 1378, 1325, 1279, 1243, 1212, 1176, 1145, 1109, 850, 798, 767, 726, 648 cm^{-1}. UV (film): λ_{max}, nm (α_A) 486 (8.46 μm^{-1}). T_g (DSC): 227 °C. T_d (TGA): 402 °C (5wt % loss). GPC (polystyrene equivalent): M_n = 28,700, PDI = 1.65. Anal. Calcd for $C_{54}H_{31}N_7O_8$: C, 71.60; H, 3.45; N, 10.82. Found: C, 71.89; H, 3.61; N, 11.03.

TMEG-NBT-Stil (33). This material was prepared from **16** and **28** and obtained as a dark-orange solid in 94% yield. ^{1}H NMR (NMP-d_9): δ 9.93 (s, 1H, Ar), 9.33 (d, 2H, J = 8 Hz, Ar), 9.14−9.10 (m, 3H, Ar), 8.97−8.86 (m, 3H, Ar), 8.69−8.60 (m, 3H, Ar), 8.44−8.37 (m, 5H, Ar), 8.11 (d, 4H, J = 8 Hz, Ar), 7.89 (d, 2H, J = 8 Hz, Ar), 5.69 (s, 4H, CH_2). IR (film, NaCl): 3478, 3074, 2997, 1791, 1724, 1590, 1517, 1476, 1440, 1388, 1341, 1284, 1248, 1217, 1186, 1124, 1093, 824, 803, 736, 643 cm^{-1}. UV (film): λ_{max}, nm (α_A) 458 (15.26 μm^{-1}). T_g (DSC): 262 °C. T_d (TGA): 370 °C (5wt % loss). GPC (polystyrene equivalent): M_n = 21,000, PDI = 2.15. Anal. Calcd for $C_{47}H_{27}N_5O_{10}S$: C, 66.12; H, 3.19; N, 8.20. Found: C, 66.34; H, 3.06; N, 8.17.

TMEG-NO2-Stil (34). This material was prepared from **14** and **28** and obtained as an orange solid in 98% yield. ^{1}H NMR (NMP-d_9): δ 9.34 (d, 2H, J = 8 Hz, Ar), 9.18 (s, 2H, Ar), 9.04−8.95 (m, 4H, Ar), 8.73 (d, 2H, J = 8 Hz, Ar), 8.55 (d, 2H, J = 8 Hz, Ar), 8.47−8.21 (m, 6H, Ar), 8.07 (d, 4H, J = 8 Hz, Ar), 7.93 (d, 2H, J = 8 Hz, Ar), 5.70 (s, 4H, CH_2). IR (film, NaCl): 3472, 2986, 1786, 1729, 1584, 1512, 1429, 1383, 1347, 1326, 1279, 1253, 1217, 1171, 1093, 974, 850, 798, 731, 529 cm^{-1}. UV (film) λ_{max}, nm (α_A) 430 (14.16 mm^{-1}). T_g (DSC): 237 °C. T_d (TGA): 410 °C (5wt % loss). GPC (polystyrene equivalent): M_n = 25,100, PDI = 2.60. Anal. Calcd for $C_{46}H_{28}N_4O_{10}$: C, 69.35; H, 3.54; N, 7.03. Found: C, 69.24; H, 3.68; N, 7.38.

SHG Measurements and Film Preparation. Molecular hyperpolarizabilities were measured at 1907 nm in chloroform solution using the electric field-induced second-harmonic generation (EFISH) techniques previously described.[18] After using second-harmonic generation to measure β (-2ω; ω, ω) and extrapolating this value to zero frequency,[19] this quantity was then converted to an electrooptic-hyperpolarizability $\beta(-\omega; \omega, 0)$ at 1300 nm, yielding the reported chromophore β values, designated as $\beta^{EO}{}_{1300}$. All β values are referenced to the currently accepted d_{11} value of 6.7×10^{-10} esu for quartz[20] at 1907 nm. EFISH data for compounds **20**,[14] **21**,[21] **22**,[22] **23**,[14] **25**,[21] and **26**[21] are taken from the literature.

Prior to spin casting, polymers were dissolved in 1,1,2,2-tetrachloroethane (6−13 wt %) and filtered through a 0.45 μm Teflon membrane filter. For thermal studies, films were cast on 1 in. quartz disks, and for poling studies, 1 in. × 3 in. × 1 mm microscope slides were used. The quartz disks and microscope slides were subjected to the cleaning procedure described below. Substrates were immersed in concentrated H_2SO_4 for 5 min, rinsed with distilled water, and placed into a distilled water spraybar for 5 min. They were then immersed in constantly refilled distilled water bath with N_2 bubbling through while the resistance was monitored until >7 ohms. Finally, the substrates were placed in a 2-propanol vapor bath for 5 min and then dried in a dry air oven (120 °C). Films were spin cast at 25° at 2000−2500 rpm. After 45 s of spinning, the film was dried under air at 75 °C for 30 min and under reduced pressure (∼20 mmHg) at 100 °C for an additional 24 h.

Polymer films were poled in a corona discharge field under N_2 using a 40 μm diameter W corona wire in a wire-to-plane geometry 1 cm above a Teflon protected, grounded Al block. The Al block allows the sample to be heated in situ while Teflon spacers on top prevent shorting. The film temperature was raised by a heating plate positioned under the Al block, and the film temperature was measured with a thermocouple placed directly on top of the polymer film. The temperature was rapidly increased to ∼50−75 °C below T_g before the corona field was applied, and the temperature was the gradually increased (∼10 °C/min) to the poling temperature (∼15 °C below T_g for the 6F-based films; 5 °C above T_g for the TMEG-DA-based films.) The corona field was then maximized (∼4.5−6.0 kV) while the current through the film was monitored. Small increases in corona field strength resulted in large jumps in the current. Although currents as high as 20 μA could be applied with only minor visible damage, currents in the range of 2.0−3.5 μA generated the largest NLO responses. Films were maintained at the optimal temperature and current for 30 min whereupon the heating block was cooled to room temperature in the presence of the field. Finally, the poling field was removed.

SHG experiments were performed with a p-polarized beam at the fundamental frequency of a mode-locked Q-switched Nd:YAG laser (Quantronix 527CWYLF) operating at 10 Hz with 8 ns subpulses in each pulse train as described previously.[23] The sample was oriented perpendicular to the beam, and the signal optimized by rotation to Brewster's angle. SHG signals from the p-polarizer were accumulated using a photomultiplier tube and averaged with a boxcar averager. A 4.65 mm Y-cut quartz plate was used as the reference, and the nonlinearities of the films (reported as $\chi^{(2)}$ values) were calculated as described by Knoesen et al.[23] The estimated uncertainty in $\chi^{(2)}$ values is ±5%.

(18) Moylan, C. R.; Miller, R. D.; Twieg, R. J.; Betterton, K. M.; Lee, V. Y.; Matray, T. J.; Nguyen, C. *Chem. Mater.* **1993**, *5*, 1499.

(19) Moylan, C. R.; Twieg, R. J.; Lee, V. Y.; Miller, R. D.; Volksen, W.; Thackara, J. I.; Walsh, C. A. *SPIE Proc.* **1994**, *2285*, 17.

(20) Moylan, C. R.; Swanson, S. A.; Walsh, C. A.; Thackara, J. I.; Twieg, R. J.; Miller, R. D.; Lee, V. Y. *SPIE Proc.* **1993**, *2025*, 192.

(21) Moylan, C. R.; Miller, R. D.; Twieg, R. J.; Lee, V. Y. In *Polymers for Second-Order Nonlinear Optics*; Lindsay, G. A., Singer, K. D., Eds.; ACS Symposium Series 601; American Chemical Society: Washington, DC, 1995; pp 66−81.

(22) Miller, R. D.; Burland, D. M.; Jurich, M.; Lee, V. Y.; Moylan, C. R.; Twieg, R. J.; Thackara, J.; Verbiest, T.; Volksen, W.; Walsh, C. A. In *Polymers for Second-Order Nonlinear Optics*; Landsay, G. A.; Singer, K. D., Eds.; ACS Symposium Series 601; American Chemical Society: Washington, DC, 1995; pp 130−146.

(23) Mortazavi, M. A.; Knoesen, A.; Kowel, S. T.; Higgins, B. G.; Dienes, A. *J. Opt. Soc. Am. B* **1989**, *6*, 733.

Scheme 1. Synthesis of Imbedded-Head Chromophore Precursors

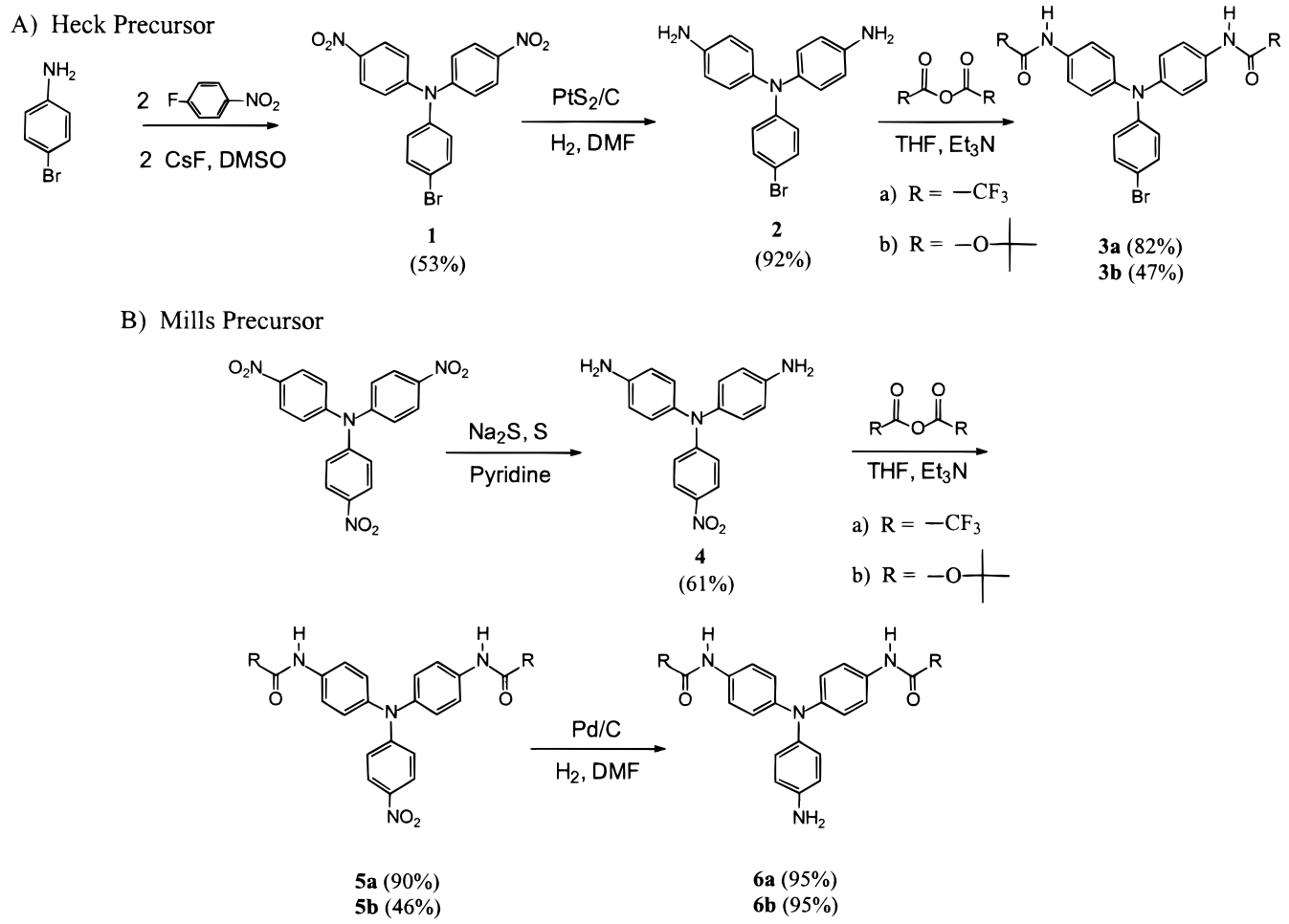

Results and Discussion

Chromophore Synthesis. A series of novel diamine-functionalized chromophores suitable for incorporation into the main chains of high T_g polyimide systems were prepared as depicted in Schemes 1−4. The overall synthetic strategy is convergent in which the protected diamine portion and the electron-withdrawing fragments are prepared separately, followed by coupling and deprotection to yield the desired diamino-substituted NLO chromophore.

Since both azo- and stilbene-based NLO chromophores were of interest, the diamine precursor portion was functionalized with either a 4-bromophenyl group suitable for a subsequent Pd-catalyzed Heck-type[24] reaction to afford the stilbene, or with a 4-aminophenyl group for a subsequent Mills-type[25] condensation when the azo derivative was desired. For the former, 4-bromoaniline was first coupled with 4-fluoronitrobenzene in the presence of CsF to yield dinitrobromo derivative **1** (Scheme 1A), and the resulting dinitro compound was then reduced to the diamine **2** using PtS_2/C to avoid hydrogenolysis of the aryl halide.[26] The diamines were protected either as the bis-trifluoroacetamide (TFA) **3a** or the bis-*tert*-butoxy carbonyl (*t*-BOC) derivative **3b**. In general, TFA was found to be the most useful protecting group for the diamines; however, in certain cases the *t*-BOC derivative also proved useful, particularly if base sensitivity of the final chromophore is an issue.

For the Mills coupling to produce the azo derivative (Scheme 1B), initially tris(4-nitrophenyl)amine was reduced to tris(4-aminophenyl)amine by catalytic hydrogenation and this coupled to yield a mixture of the mono-, di-, and trifunctionalized materials. This route provides the desired product in low yield, so we resorted to the selective protection of two amino substituents, leaving the third available for the azo formation. However, low yields and complicated purifications characterize this approach. To overcome this difficulty, the controlled partial reduction of tris(4-nitrophenyl)amine to bis(4-aminophenyl)(4-nitrophenyl)amine **4** using sodium sulfide, sulfur, and pyridine was accomplished. Litvinenko et al.[27] reported that 1 h under these conditions yielded the monoreduced product (in 93% yield). Careful monitoring showed that extending the reaction time to 3 h results in an optimized diamine yield (61%) with essentially no triamine. Diamine **4** was then first protected as either the TFA (**5a**) or *t*-BOC (**5b**) derivative, followed by subsequent reduction of the remaining nitro substituent to the primary amines, **6a** and **6b** respectively, using Pd/H_2.

(24) Heck, R. F. *Org. React.* **1982**, *27*, 345.
(25) Boyer, J. H. In *The Chemistry of the Nitro and Nitroso Groups*; Feuer, H., Ed.; Interscience: New York, 1969; Part 1, pp 278−283.
(26) Greenfield, H. *Ann. NY Acad. Sci.* **1967**, *145*, 108.
(27) Litvenenko, L. M.; Popova, R. S.; Popov, A. F.; Gorokhovskii, G. B. *J. Org. Chem., USSR* (*Engl. Transl.*) **1971**, *7*, 808.

Scheme 2. Synthesis of Chromophore Acceptor Moieties

A) Vinyl Substituted Precursors

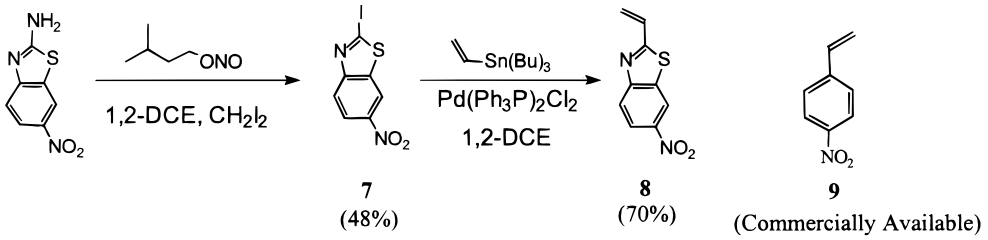

7 (48%) **8** (70%) **9** (Commercially Available)

B) Nitroso Substituted Precursor

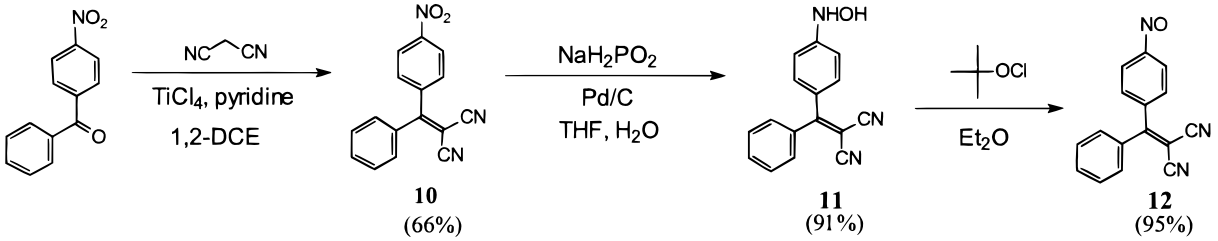

10 (66%) **11** (91%) **12** (95%)

Pd-catalyzed Heck coupling reactions are more efficient when the olefin is substituted with electron-withdrawing (EWG) substituents.[28] Thus, we utilized either commercially available 4-nitrostyrene **9** or the synthesized 2-vinyl-6-nitrobenzothiazole **8** (Scheme 2). The latter was prepared by diazotization of 2-amino-6-nitrobenzothiazole with isoamylnitrite in 1,2-dichloroethane followed by in situ iodo substitution[29] using diiodomethane to afford 2-iodo-6-nitrobenzothiazole **7**. The Pd-catalyzed Stille[30] reaction of **7** with tributylvinyltin yielded the desired 2-vinyl-6-nitrobenzothiazole **8** in 34% yield overall. Both of the olefins, 4-nitrostyrene **9** and 2-vinyl-6-nitrobenzothiazole **8**, were then coupled to the protected diamine precursor **3a** using palladium(II) acetate, tris-*o*-tolyl phosphine in DMF/Et_3N to afford the respective trifluoroacetamido-protected chromophores **13a** and **15** (Scheme 3). Deprotection with potassium carbonate in MeOH/H_2O followed by flash chromatographic purification yielded desired diamine chromophores **14** and **16**, respectively. To demonstrate the potential synthetic utility of the *t*-BOC protecting group, **3b** was also coupled to 4-nitrostyrene **9** to afford protected chromophore **13b**. Facile deprotection using trifluoroacetic acid in methanol yields the same diamine **14** as obtained via the trifluoroacetamido route. Because of the robustness of the 6-nitrobenzothiazole group, particularly toward base, only the TFA protecting group was utilized in this case.

For the azo chromophore, required nitroso derivative **12** was generated via the Knovenagel[31] condensation of 4-nitrobenzophenone with malononitrile in the presence of titanium (IV) tetrachloride to give 2-(4-nitrophenyl)-2-phenyl-1,1-dicyanoethylene **10** (Scheme 2b). Selective reduction to the hydroxylamine[32] **11** was accomplished with sodium hypophosphite and Pd/C. Utilizing our previously described homogeneous oxidation procedure employing *tert*-butyl hypochlorite,[33] nitroso-functionalized chromophore precursor 2-(4-nitrosophenyl)-2-phenyl-1,1-dicyanoethylene **12** is produced in 95% yield. Condensation of **6a** with the nitroso derivative **12** yielded the azo compound **19** (Scheme 4). However **19** could not be deprotected using the usual techniques (K_2CO_3/MeOH/H_2O) due to the extreme sensitivity of the dicyanoethylene functionality to basic reaction conditions. The Mills condensation of **12** and **6b** was accomplished in tetrahydrofuran/acetic acid to yield protected chromophore **17** in 58% yield. Deprotection using 3 M HCl in ethyl acetate yields desired diamine **18**.

Table 1. Chromophore Thermal Stability Data

chromophore	T_d[a] (°C) via DSC	TGA (°C) at 5wt % loss
TFA-NO2-Stil (**13a**)	320	340
BOC-NO2-Stil (**13b**)	225	235
DA-NO2-Stil (**14**)	315	200
TFA-NBT-Stil (**15**)	362	290
DA-NBT-Stil (**16**)	327	325
TFA-DCVPh-Azo (**19**)	388	380
BOC-DCVPh-Azo (**17**)	295	225
DA-DCVPh-Azo (18)	293	287

[a] T_d stands for the onset decomposition temperature.

Chromophore Thermal Characteristics. The overall thermal stability of an NLO chromophore-containing polymer is determined by the intrinsic chromophore thermal stability as modified by/in combination with the associated polymer structure. We have characterized the thermal stability of the present chromophores containing both free and derivatized amino substituents. For the present purposes, the protected diamines are more representative of the polyimide chemical environment. The thermal properties of the diamines (**14**, **16**, and **18**) and their derivatives are reported in Table 1. DSC data were recorded at a heating rate of 20 °C/min, and

(28) Spencer, A. *J. Organomet. Chem.* **1983**, *258*, 101.
(29) Based on: Nair, V.; Richardson, S. G. *Synthesis* **1982**, *8*, 670.
(30) Stille, J. K. *Angew. Chem., Int. Ed. Engl.* **1986**, *25*, 508.
(31) Based on: Vorob'eva, S. L.; Berzina, T. S. *J. Chem. Soc. Perkin Trans. 2* **1992**, 1133.
(32) Entwistle, I. D.; Gilkerson, T.; Johnstone, R. A. W.; Telford, R. P. *Tetrahedron* **1978**, *34*, 213.
(33) Davey, M. H.; Lee, V. Y.; Miller, R. D.; Marks, T. J. *J. Org. Chem.* **1999**, *64*, 4976.

Scheme 3. Preparation of Stilbene Chromophore Derivatives via Heck Coupling

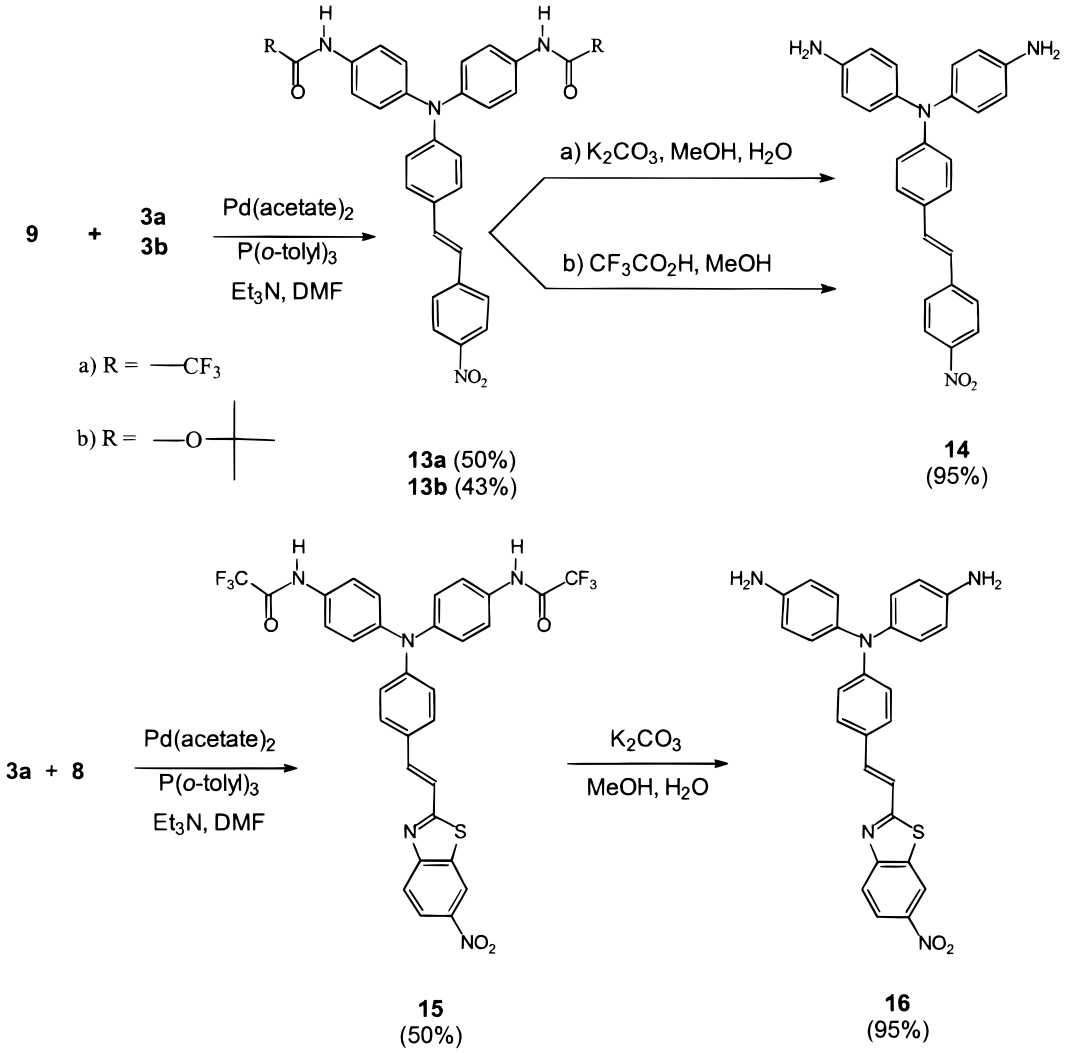

decomposition temperatures are defined as the onset decomposition temperatures of the respective chromophores. This temperature is calculated from the intersection of the tangent to the steepest slope of the decomposition exotherm with the adjusted baseline. TGA data were also recorded at a heating rate of 20 °C/min, and the temperature where 5% weight loss occurs was recorded.

For nitro-stilbene-containing chromophores **13a**, **13b**, and **14** (Table 1), trifluoroacetamido derivative **13a** has the highest onset decomposition temperature (320 °C) as measured by DSC. Diamine **14** also appears to be quite stable with a decomposition temperature of 315 °C; however, TGA shows a 5% weight loss at 200 °C. This discrepancy can be resolved through the examination of the DSC data. The diamine melts at about 160 °C followed by an immediate decomposition to some unknown compound, which exhibits another melting transition at 194 °C. During this process, some material is lost, and the TGA shows a change in weight. The high decomposition temperature is a result of this unknown decomposition product. Finally, *t*-BOC derivative **13b** decomposes at the lowest temperature, losing isobutylene around 225 °C[34] to produce the corresponding diamine, which immedately decomposes. The bis-trifluoroacetamido derivative is probably the most appropriate model for the chromophore molecule incorporated into a polyimide, and it is quite thermally stable. In our experience, free diamine-containing chromophores tend to be considerably less stable than either the amide or imide derivatives.

Since we have not prepared the corresponding *t*-BOC derivative of the 6-nitrobenzothiazole stilbene chromophore (NBT-Stil), thermal stabilities are reported only for the corresponding diamine and bis-trifluoroacetamido derivatives. Bis-trifluoroacetamido derivative **15** exhibits an onset decomposition temperature of 362 °C while that of the diamine **16** is again somewhat lower (∼327 °C). Dynamic TGA data for trifluoroacetamido derivative **15** show that this material suffers ∼5% weight loss at temperatures as low as 290 °C.

We have also studied the thermal stabilities of chromophores containing the dicyanovinylphenyl substituent (**17**, **18**, and **19**; Table 1), although only azo derivatives were prepared. Bis-trifluoroacetamido derivative **19** is exceptionally stable with a measured onset decomposition temperature of 388 °C. TGA studies confirm this stability with 5% weight loss occurring around 380 °C. As expected, the *t*-BOC (**17**) and diamine (**18**) derivatives are both considerably less stable than

(34) (a) Rawal, V. H.; Jones, R. J.; Cava, M. P. *J. Org. Chem.* **1987**, *52*, 19. (b) Bykhovskaya, E. G.; Gontar', A. F.; Knunyants, I. L. *Bull. Acad. Sci. USSR Div. Chem. Sci.* (*English Transl.*) **1984**, *33*, 399.

Scheme 4. Preparation of Azo Chromophore Derivatives via Mills Coupling

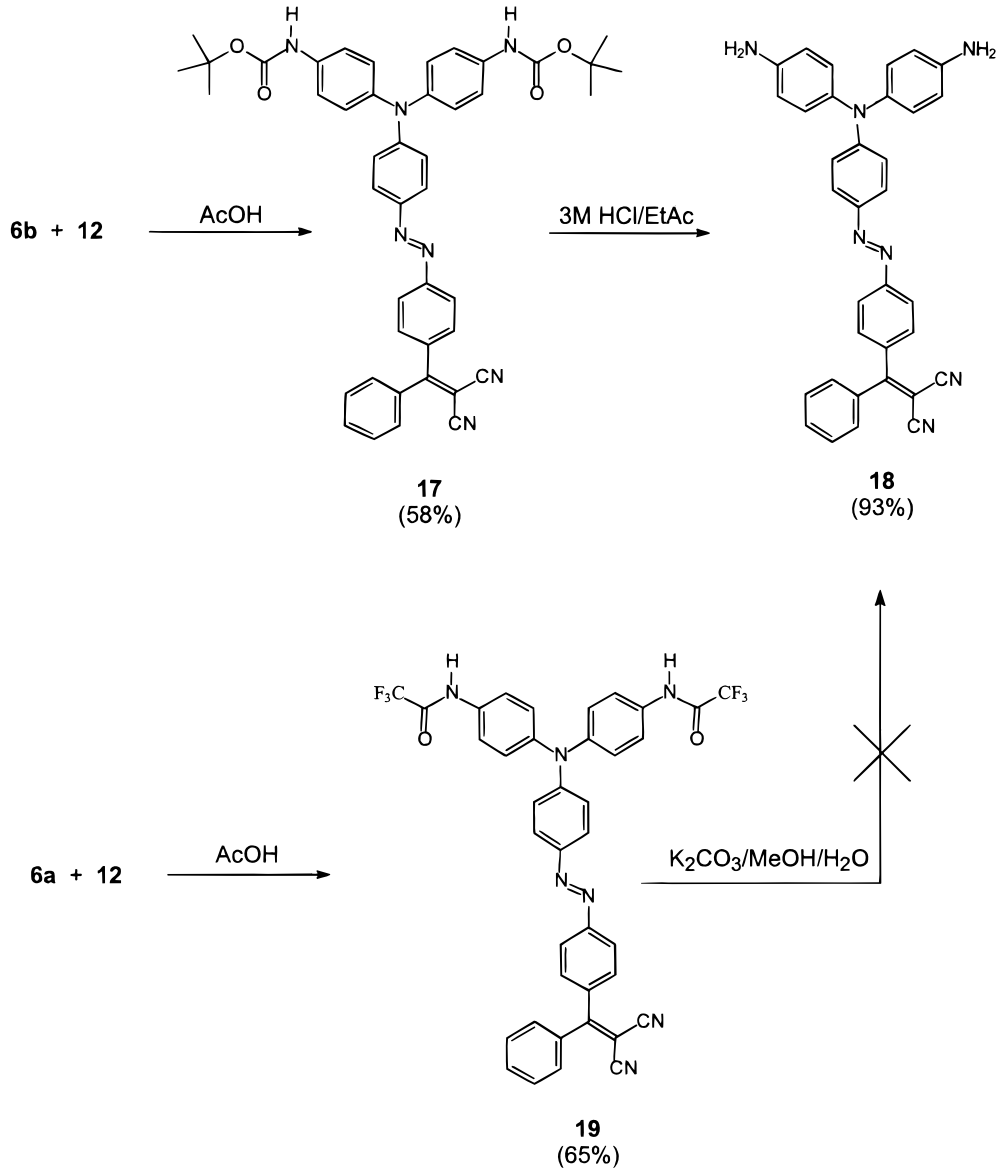

the TFA derivatives, exhibiting onset decomposition temperatures of 297 and 293 °C, respectively. As before, the *t*-BOC (**17**) derivative appears to undergo thermal deprotection below 250 °C to produce the corresponding diamine, which then decomposes at 295 °C as observed for respective diamine.

The thermal stabilities of bis-trifluoroacetamido derivatives **13a**, **15**, and **19** provide some insight into the type of polyimide structure which might be appropriate for poled NLO polymer studies. Here chromophore stability at or near the projected polymer T_g is required. In this regard, donor-embedded polyimides derived from hexafluoroisopropylidene diphthalic anhydride (6FDA; **27**; Figure 1), while often soluble in the imidized form, exhibit substantially higher T_g values than those derived from the 2-(1,3-dioxoisobenzofuran-5-ylcarbonyloxy)ethyl 1,3-dioxoisobenzofuran-5-carboxylate (TMEG-DA; **28**; Figure 1) due to the presence of an aliphatic spacer group in the latter. Since the polyimide derived from 6FDA (**27**) and bis(4-aminophenyl)[4-((4-nitrophenyl)diazenyl)phenyl]amine (Figure 2) has a $T_g \approx 350$ °C,[5a,b] polyimides of this type will be suitable for only the most thermally stable chromophores.

On the basis of these criteria, we predict that the DCVPh-Azo chromophore **18** is appropriate for either the 6F- or TMEG-derived polyimides while the TMEG polyimide is more suitable for less thermally stable NBT-Stil chromophore **16**. The improved thermal stability of the NO2-Stil chromophore **14** (T_d = 320 °C), suggests it may be appropriate for either the 6F- or TMEG-based polyimides.

EFISH Determination of Chromophore Optical Nonlinearities. To compare the optical nonlinearities of the present chromophores, molecular hyperpolarizabilities were measured using EFISH techniques.[18,35] For these measurements, γ is neglected, hence the uncertaintly in β values is $\sim\pm 3\%$.[21] Measurements were performed at 1907 nm in $CHCl_3$, utilizing model chromophores (Figure 3) devoid of the arylamino substituents required for polymerization. The addition of the arylamino substituents significantly increases the complexity of the synthesis, and since these peripheral substituents are expected to contribute little to the hyperpolarizability, the focus on model compounds is

(35) Levine, B. F.; Bethea, C. G. *J. Chem. Phys.* **1975**, *14*, 1447.

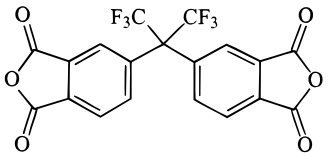

27

6FDA

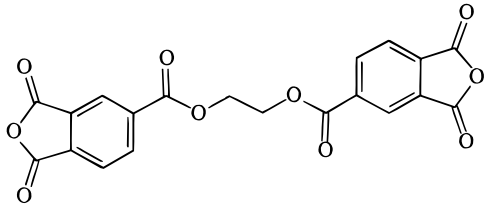

28

TMEG-DA

Figure 1. Anhydrides used in embedded chromophore polyimide syntheses.

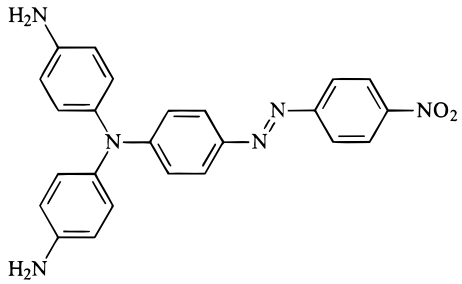

bis(4-aminophenyl)(4-((4-nitrophenyl)diazenyl)phenyl)amine

Figure 2. Diamine monomer used for high T_g polyimides.

justifiable. While the λ_{max} values of the model chromophores are not expected to precisely match those of the chromophore incorporated into the polymer backbone, the values are reasonably close—usually within 20 nm. Thus, the EFISH data in Table 2 for the model chromophores should provide a reasonable indication of the second-order response properties of the final chromophore-embedded molecules. The calculated quantity $\mu\beta_{1300}(-\omega; \omega, 0)$ is estimated from the EFISH-derived hyperpolarizability [$\beta_0(-2\omega; \omega, \omega, 0)$], transformed to $\beta^{EO}{}_0$ $(-\omega; \omega, 0)$ and extrapolated to 1300 nm, using the standard two-level model[36,37] and the measured dipole moments. The calculation of $\mu\beta_{1300}(-\omega; \omega, 0)$ requires both a conventional correction for the measured molecular hyperpolarizability $(-2\omega; \omega, \omega,)$ determined by EFISH experiments and an accurate value for the nonlinearity of the quartz standard.[19] In addition to $\mu\beta_{1300}(-\omega; \omega, 0)$, a reduced nonlinearity[21] (i.e., $\mu\beta_{1300}(-\omega; \omega, 0)$/MW) is also presented in Table 2 as an appropriate figure of merit.

Chromophore EFISH, linear optical, and thermal stability data (Figure 3) are summarized in Table 2, with the most relevant data being the reduced nonlinearity, the decomposition temperature, T_d, and the chromophore λ_{max} measured by UV−vis spectroscopy. The data are grouped according to similarities of electron-withdrawing groups (EWG).

For the nitrophenyl EWG, previously described[5a,b] azo chromophore **21** (Figures 2 and 3) is compared to the new stilbene derivative **20**. Since stilbene chromophore **20** absorbs at substantially shorter wavelengths (~50 nm) than azo derivative **21**, the reduced nonlinearity is only slightly more than half that of the latter, as expected from the reduced resonance enhancement anticipated from the optical spectra. For the 6-nitrobenzothiazole EWG (**22** and **23**), although the onset decomposition temperature is higher for stilbene derivative **22** than for azo counterpart **23**, the stilbene absorption maximum is blue-shifted by >90 nm, and the calculated reduced nonlinearity is 1.70 vs 3.10 for azo chromophore

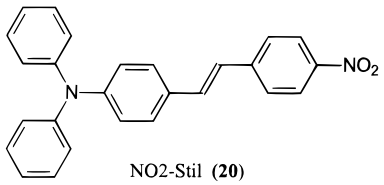

NO2-Stil (**20**)

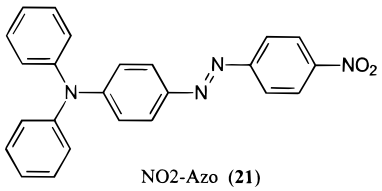

NO2-Azo (**21**)

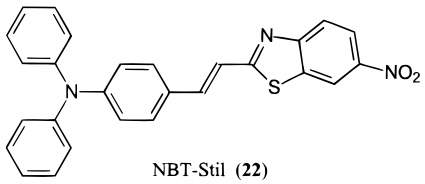

NBT-Stil (**22**)

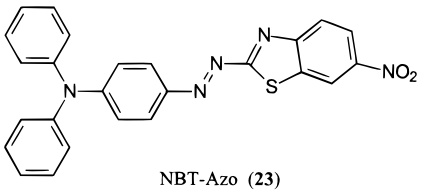

NBT-Azo (**23**)

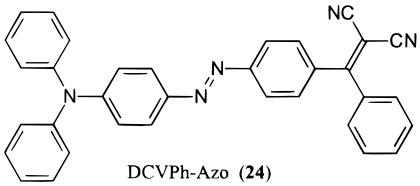

DCVPh-Azo (**24**)

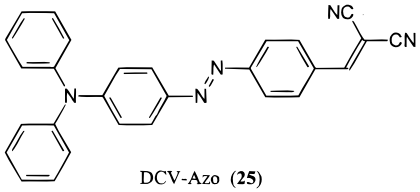

DCV-Azo (**25**)

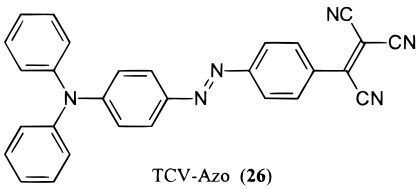

TCV-Azo (**26**)

Figure 3. Model chromophores used for EFISH comparison.

Table 2. EFISH and Thermal Properties of Model Chromophore Moieties

chromophore	μ	β_0 (-2ω; ω, ω)	$\beta^{EO}{}_{1300}$	$\mu\beta^{EO}{}_{1300}$	$\mu\beta_{1300}$/MW	T_d (°C)	λ_{max} (nm)	ref
NO2-Stil (**20**)	4.75	37.3	88	418	1.10	358	436	14
NO2-Azo (**21**)	5.87	54.3	135	792	2.01	393	486	21
NBT-Stil (**22**)	5.48	57.2	138	756	1.70	367	458	22
NBT-Azo (**23**)	7.21	71.8	194	1398	3.10	356	550	14
DCVPh-Azo (**24**)	8.20	82.5	104	853	1.71	412	494	this work
DCV-Azo (**25**)	6.74	149	202	1361	3.20	383	526	21
TCV-Azo (**26**)	7.11	259	391	2780	6.17	364	602	21

[a] All EFISH measurements performed in $CHCl_3$ at 1907 nm. [b] Allo $\mu\beta$ values are expressed in 10^{-30} esu.

23. While we were interested in both the stilbene and azo derivatives, we were unable to prepare the corresponding functionalized azo chromophore containing the 6-nitrobenzothiazole unit, hence only the 6-nitrobenzothiazole stilbene chromophore was incorporated into polyimide structures.

The EFISH data in Table 2 for cyano-based chromophores **24**, **25**, and **26** all refer to the respective azo derivatives. While tricyanovinyl-substituted chromophore **26** absorbs at longest wavelength (λ_{max} = 602 nm) and displays an impressive reduced nonlinearity of 6.17, the α-cyano (i.e., α to the aromatic ring) substituent in the tricyano group leads to reactivity with nucleophiles,[3e] resulting in chemical instability. Replacement of the α-cyano substituent with H yields dicyanovinyl chromophore **25**. Although this chromophore absorbs at considerably shorter wavelengths than tricyano analogue **26**, it still exhibits a substantial reduced nonlinearity (3.20) and is more thermally stable (Table 2). The dicyanovinyl substituent, however, like the tricyanovinyl group, is still prone to nucleophilic attack. Substitution at the α-position of the EWG with phenyl (e.g., **24**) markedly increases thermal and chemical stability.[38,39] However, the price paid is a significant decrease in the reduced nonlinearity (1.71). Undoubtedly the phenyl substituent is substantially twisted from coplanarity with the rest of the chromophore EWG. This distortion would be expected to adversely affect chromophore nonlinearity. The crystal structure of a related chromophore containing an α-phenyl substituent also exhibits significant twisting.[3e]

The present EFISH measurement studies reveal somewhat lower $\mu\beta$ values (~1000 × 10^{-48} esu) than several high hyperpolarizability/high dipole moment ($\mu\beta \cong$ 10 000−18 000 × 10^{-48} esu) chromophores recently reported;[3] however, the latter are complicated by lower thermal stabilities and may be more susceptible to oxidative or photochemical degradation.[4] Compared to other high thermal stability chromophore systems,[5] the hyperpolarizabilities of the present chromophores are approximately the same order of magnitude.

Embedded Chromophore Polymer Synthesis and Thermal Characterization. For the synthesis of second-order NLO polyimides, two commercially available dianhydrides were selected (6FDA, **27** and TMEG-DA, **28**; Figure 1). The selection of **27** and **28** was motivated by the generally improved solubility of polyimides derived from these anhydrides and the expected high T_g values for the chromophore-embedded polyimides. The intrinsic structural flexibility of TMEG-DA **28** usually results in polyimide derivatives having lower T_g values than those prepared using more rigid 6FDA **27**. The polyimide syntheses were accomplished by straightforward condensation sequences via the corresponding polyamic acids, and the structures of the fully imidized products are depicted in Figure 4.

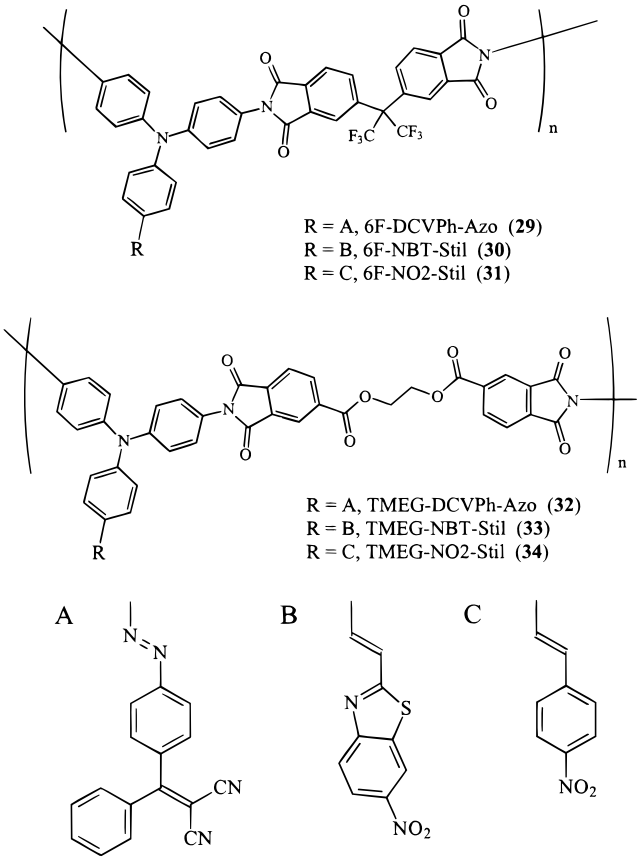

Figure 4. Chromophore-embedded polyimides synthesized in this study.

To estimate the thermal stability of each NLO chromophore-embedded polymer, a thermal analysis protocol having predictive utility was developed. For each polymer synthesized, five different measurements are employed as discussed below.

(i) T_g of the polymer relative to the chromophore decomposition temperature is a critical feature for efficient electric field poling. Since both the measured T_g and T_d are dependent upon the instrumental heating rate, a ramp rate of 20 °C/min is selected as standard for all measurements.

(ii) The onset decomposition temperature, T_d (measured by DSC), of the polymer is determined at a heating ramp rate of 20 °C/min and is calculated in the same manner as described above for the individual chromophores.

(36) Oudar, J.; Chemla, D. *J. Chem. Phys.* **1977**, *66*, 2664.
(37) Oudar, J.; Zyss, *J. Phys. Rev. A* **1982**, *26*, 2016.
(38) Rao, V. P.; Jen, A. K.-Y.; Cai, Y. *Chem. Commun.* **1996**, 1237.
(39) Ermer, S.; Lovejoy, S. M.; Leung, D. S.; Warren, H.; Moylan, C. R.; Twieg, R. J. *Chem. Mater.* **1997**, *9*, 1437.

Table 3. Chromophore-Embedded Polyimide Thermal Properties

	6F-DCVPh-Azo (**29**)	6F-NBT-Stil (**30**)	6F-NO2-Stil (**31**)	TMEG-DCVPh-Azo (**32**)	TMEG-NBT-Stil (**33**)	TMEG-NO2-Stil (**34**)
T_g (DSC)	313	N/A	312	227	262	237
T_d (DSC, onset)	420	360	375	392	358	350
T_d^5 (TGA)	475	415	420	402	370	410
T_d^0 (DSC, onset)	364	340	328	330	298	317
T_d^{10} (UV−vis)	355	284	306	291	266	292

[a] All temperatures are presented in Celsius.

(iii) The equilibrium onset decomposition temperature, T_d^0, is determined by DSC extrapolated to a nominal heating ramp rate of 0 °C/min to mediate the effects of heating rate. This parameter is determined by extrapolating the onset decomposition temperatures obtained at various heating rates to 0 °C/min. This quantity provides the most accurate representation of the true polymer thermal stability. In some cases, the decomposition temperature measured at 20 °C/min deviates substantially from the extrapolated line. When this occurs, the data point at 20 °C/min is usually neglected since very high heating rates tend to overestimate chromophore/polymer stability.

(iv) The weight loss decomposition temperature, T_d^5 (TGA), is defined as the point at which 5% weight loss has occurred in the polymer at a heating rate of 20 °C/min. This often occurs substantially above the onset decomposition temperatures determined by DSC.

(v) A final measurement defined as T_d^{10}, represents the temperature at which the NLO polymer loses 10% of the original optical absorbance at λ_{max}, as determined by variable temperature UV−vis spectroscopy of the film. While the aforementioned measurements (i−iv) assay the thermal properties of the entire chromophore + polymer system, T_d^{10} is specific to the chromophore unit itself contained in the polymer matrix environment. Since the nonlinearity of the polymer achieved upon poling is provided primarily by the oriented chromophore moieties, this is a critical measurement. The measurement is performed by first casting a polymer film onto a quartz substrate, briefly drying to remove solvent, and finally measuring the UV−vis spectra at various temperatures. At the absorption λ_{max}, the optical density is monitored as the polymer film is stepped through a series of temperatures, each increasing in 25 °C intervals. The isothermal heating period at each temperature is maintained for 30 min. Finally, a plot of chromophore absorbance (normalized to the initial measurement) versus temperature is plotted and the temperature at which the normalized absorbance falls to 0.9 is defined as the T_d^{10}.

On the basis of the measured thermal properties of the NLO chromophore/polymer system, poling conditions are selected. Empirical observations suggest that in most cases the chromophore/polymer system should be stable to at least within 20 °C of T_g to prevent significant decomposition during poling, since poling must be conducted near but slightly below the polymer T_g to be efficient. The present TMEG-DA-based polymers are anomalous in this regard since it is found empirically that materials of this type are actually most efficiently poled 5−10 °C above T_g.

As shown in Table 3, 6F-NO2−Stil (**31**; Figure 4) and TMEG-NBT-Stil (**33**; Figure 4) exhibit thermal stabilities, as measured by the aforementioned thermal analysis protocol, which are compatible with the proposed poling guidelines. However, examination of the T_d^{10} data, as determined by variable-temperature UV−vis spectroscopy, raises some concern with regard to the actual thermal longevity of the chromophore structures under poling conditions. For 6F-NO2-Stil, T_d^{10} is 306 °C and the polymer T_g is 312 °C, while for TMEG-NBT-Stil, T_d^{10} is 266 °C and T_g is 262 °C. In these cases, the poling time was deliberately shortened in an attempt to mitigate possible thermal instability effects. In the case of the TMEG-NO2−Stil (**34**), TMEG-DCVPh-Azo (**32**), and 6F-DCVPh-Azo (**32**) polymers, the measured T_g values are significantly lower than any of the thermal decomposition temperatures, and therefore negligible decomposition would be expected during poling. Finally, for the 6F-NBT-Stil, no T_g signature could be detected by DSC. This material appears to decompose before reaching T_g, and not unexpectedly, poling produces no measurable polar orientation (vide infra).

Processability is also an issue for NLO polymers since low loss, optical-quality films are required for device applications. While the 6F-based polymers exhibit excellent solubility in common organic solvents (THF, anisole, 1,2-dichloroethane (DCE), 1,1,2,2-tetrachloroethane (TCE)) and spin-coating properties, the corresponding TMEG-DA-based materials are much less soluble. Although the TMEG-NO2-Stil polymer (**34**) has limited solubility in NMP, which allows UV and IR spectroscopic measurements, good optical quality films of ≥ 1 μm in thickness could not be prepared. TMEG-NBT-Stil (**33**) is slightly more soluble in TCE and NMP initially; however, the solutions frequently gel (thermally reversible) at greater than 2 wt % loading if left standing for extended periods. The difficulty in spinning good films due to this gelation process results in micrometer thick films of questionable optical quality due to increased surface roughness and other film defects. In contrast, the TMEG-DCVPh-Azo polymer (**32**) is similar to the 6F polymers in that it is soluble, and high optical quality films can be spin cast.

Polymer Poling, NLO Response. Corona poling was carried out as described in the Experimental Section. Table 4 presents a summary of the data for the six materials in this study. The nonlinearities are reported as $\chi^{(2)}$ values and were calculated as described previously.[23] The film thickness (L_s) and ratio of the sample nonlinear response relative to quartz (I_s/I_q) are also included in the table for reference.

The NLO response data can be divided into two groups, depending upon the polymer architecture. In the case of the 6F polymers, note that 6F-NBT-Stil (**30**) could not be poled because of the high T_g and lower chromophore decomposition temperature. Attempts to pole at 275, 300, and 325 °C were conducted with no observed SHG response. The remaining two 6F poly-

Table 4. Poled Polymer Nonlinear Optical Properties

	film thickness (μm)	SHG signal response relative to quartz, I_s/I_q	$\chi^{(2)}$ (pm/V)	model chromophore $\mu\beta^{EO}{}_{1300}$ [b]	model chromophore $\mu\beta^{EO}{}_{1300}$/MW[c]	film λ_{max} (nm)
6F-NO2-Stil (**31**)	1.21	0.27	16.1	418	1.10	418
6F-NBT-Stil (**30**)	1.10	N/A	N/A	756	1.70	440
6F-DCVPh-Azo (**29**)	1.04	0.42	47.0	853	1.71	474
TMEG-NO2-Stil (**34**)	1.11	0.95	43.0	418	1.10	430
TMEG-NBT-Stil (**33**)	1.08	0.51	77.4	756	1.70	458
TMEG-DCVPh-Azo (**32**)	1.01	0.56	82.0	853	1.71	486

[a] $\chi^{(2)}$ calculations based on 1064 nm (input) and 532 nm (output). [b] EFISH measurement. [c] Reduced nonlinearity calculation.

mers (**29** and **31**) can be poled, however, and the magnitude of the NLO response is consistent with the chromophore nonlinearities determined by EFISH (Table 4); the $\chi^{(2)}$ values scale with the measured $\mu\beta_{1300}$ values, arguing that poling-induced orientational ordering is similar.

The TMEG-DA polymers all exhibit a SHG response when heated to just above T_g in the corona field. Although the measured nonlinearities largely track the chromophore EFISH data, TMEG-NBT-Stil (**33**) and TMEG-DCVPh-Azo (**32**) polymers exhibit nearly identical responses, 77.4 and 82.0 pm/V, respectively. On the basis of the EFISH data and assuming a ±3% uncertainty for measurements, we would predict a somewhat higher raw NLO response for the TMEG-DCVPh-Azo (**32**) polymer films. However, the DCVPh-Azo chromophore (**24**) molecular weight is substantially higher than that of the NBT-Stil chromophore (**22**), and consideration of the reduced nonlinearities reveals that they are nearly identical: i.e., 1.70 for the NBT-Stil based chromophore **22** and 1.71 for the DCVPh-Azo based chromophore **24** (Table 2). Thus, the measured nonlinearities of the poled polymers are consistent with the reduced nonlinearities of the constituent chromophores, as expected. It would be useful for comparison if this trend were also observable for the 6F-based polymers; however, the thermal instability of 6F-NBT-Stil polymer **30** at poling temperatures near T_g preclude this analysis, as noted above.

In comparing the measured NLO responses of the TMEG- and 6F-based polymers, for similar chromophores, the TMEG-based polymers appear to exhibit more efficient poling. This probably reflects intrinsically lower T_g values, caused by the higher degree of chain flexibility, permitting the chromophores to experience a larger range of reorientational excursions. The reduced glass transition temperatures that facilitate lower poling temperatures also lead to somewhat lower film electrical conductivities[6] and hence higher effective poling fields.

Once net chromphore orientation has been achieved in the present polyimides, it is exceptionally thermally stable. Long-term studies of the SHG response at both 25 and 100 °C for over 1000 h reveal no significant signal diminution beyond an initial small decay (Figures 5 and 6), which usually occurs within the first 48 h. Initial decay is ubiquitous in poled polymers and is usually attributed to a combination of depletion of the electrostatic surface charge, which builds up during corona poling[23] and low-energy chromophore librations.[40] The space-persistent charge can cause a higher SHG signal due to third-order effects (e.g., 2ω; ω, ω, 0). After dissipation of this charge, only a second-order

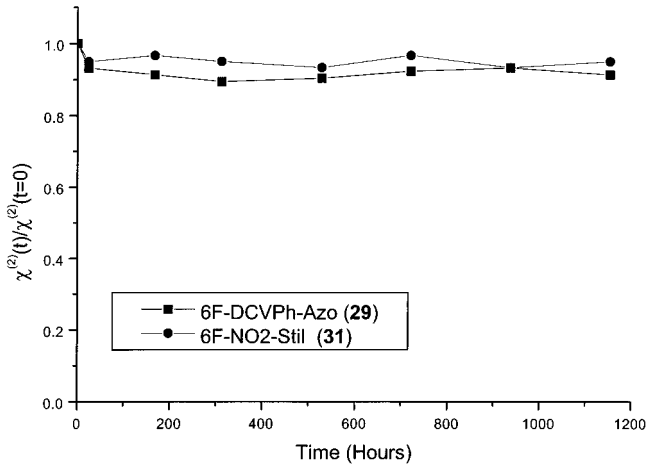

Figure 5. Normalized $\chi^{(2)}$ as a function of time for 6F-based polyimides at 100 °C in air.

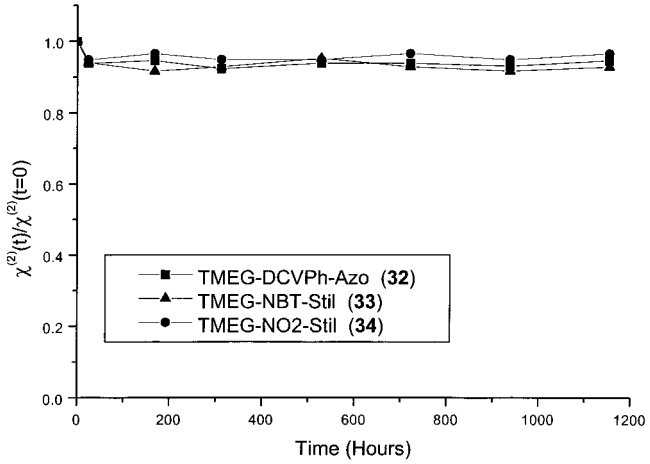

Figure 6. Normalized $\chi^{(2)}$ as a function of time for TMEG-based polyimides at 100 °C in air.

contribution from the dipole oriented material remains, and this portion of the signal remains stable. This behavior is consistent in each of the samples which could be poled.

The temporal stability of the poled polymer SHG response was also examined in situ as the samples were heated at 3 °C/min (Figures 7 and 8). As expected, all of the samples exhibit a gradual diminution of the SHG signal as the sample temperatures approach T_g. The two 6F-polymers retain ~80% of the initial response until ~225 °C, at which point rapid signal decline is evident. For the TMEG-DA polymers, TMEG-NBT-Stil (**33**)

(40) (a) Dhinojwala, A.; Wong, G. K.; Torkelson, J. M. *Macromolecules* **1993**, *26*, 5943. (b) Dhinojwala, A.; Wong, G. K.; Torkelson, J. M. *J. Chem. Phys.* **1994**, *100*, 6046.

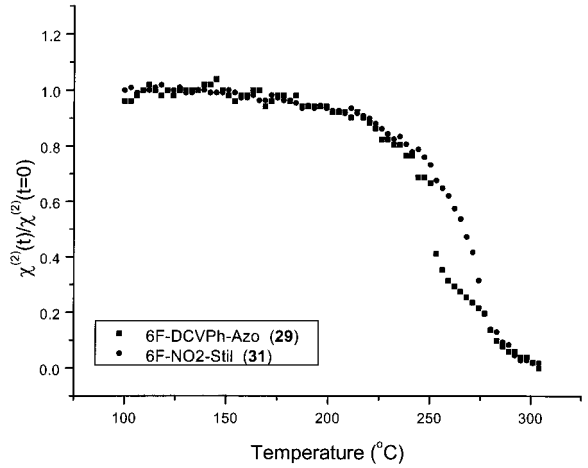

Figure 7. Thermal depoling of 6F-polymers. Temperature ramp = 3 °C/min.

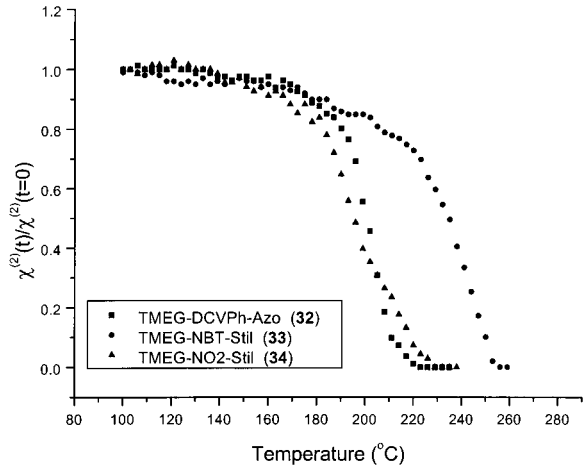

Figure 8. Thermal depoling of TMEG-polymers. Temperature ramp = 3 °C/min.

retains ~80% of the response up to ~200 °C while TMEG-DCVPh-Azo (**32**) and TMEG-NO2-Stil (**34**), which each have lower T_g's, retain ~80% of the SHG signal until ~180 °C. Extrapolation of the linear portions of the SHG curves yields an intersection near the respective polymer T_g, as expected.

Conclusions

We have developed an efficient and versatile convergent synthetic approach to stilbene- (via Heck coupling) and azo-based (via Mills coupling) donor−acceptor chromophores for incorporation into ultrahigh T_g/high thermal stability second-order NLO polyimides. This approach permits a wide variety of electron-withdrawing groups (EWG) to be incorporated into these chromophores. The synthetic protection scheme allows the introduction of both acid- and base-sensitive chromophores, and after deprotection, results in diamine-functionalized chromophores which can be readily incorporated into two types of high T_g/high thermal stability polyimide chain structures. In each case, the chromophore is incorporated into the mainchain via the donor substituents. The polymers based on the 6F-subunit, exhibit T_g's in excess of 300 °C and good processability; however, due to the higher electrical conductivity[6] and lower inherent mobility of the polymers, they do not exhibit the anticipated high levels of optical nonlinearity ($\chi^{(2)}$ = 16−48 pm/V). In contrast, polyimides based on the TMEG-DA subunit containing the same chromophore units exhibit lower T_g's (225−265 °C) but increased levels of nonlinear optical response ($\chi^{(2)}$ = 44−82 pm/V) due to greater structural mobility and poling efficiency.

For each of the present five poled polymers, once alignment has been achieved by corona poling, it remains stable for over 1000 h at both 25 °C and 100 °C. Slow heating of the samples with in situ signal monitoring shows that the TMEG polymers retain ~80% of the initial signal until 180−200 °C, while the 6F polymers retain ~80% of the initial signal until ~250 °C. Since chromophores with lower hyperpolarizabilities were utilized to ensure high levels of thermal stability while testing design concepts, the NLO responses of the present systems are not optimized for electrooptic device application. However, we have again achieved some of the highest thermal stability/polable NLO chromophore/polymer systems prepared to date. The use of the types of convergent syntheses presented here will allow for the efficient incorporation of other higher nonlinearity stilbene and azo high thermal stability chromophore modules into these polyimide mainchain systems as they are developed.

Acknowledgment. Partial financial support for this research was provided by the Northwestern Materials Research Center (MRSEC Program grant DMR-9632472) and by the Office of Naval Research through the CAMP MURI program (contract N00014-95-1-1319). We also thank Dr. P. Lundquist for performing the conductivity measurements. M. H. Davey acknowledges partial financial support from IBM Corporation as a visiting scholar.

Supporting Information Available: Detailed synthetic procedures and analytical data for compounds **1**, **2**, **4**, **7**, and **10** (4 pages). This material is available free of charge via the Internet at http://pubs.acs.org.

CM990483+